



**US Army Corps  
of Engineers®**  
Engineer Research and  
Development Center

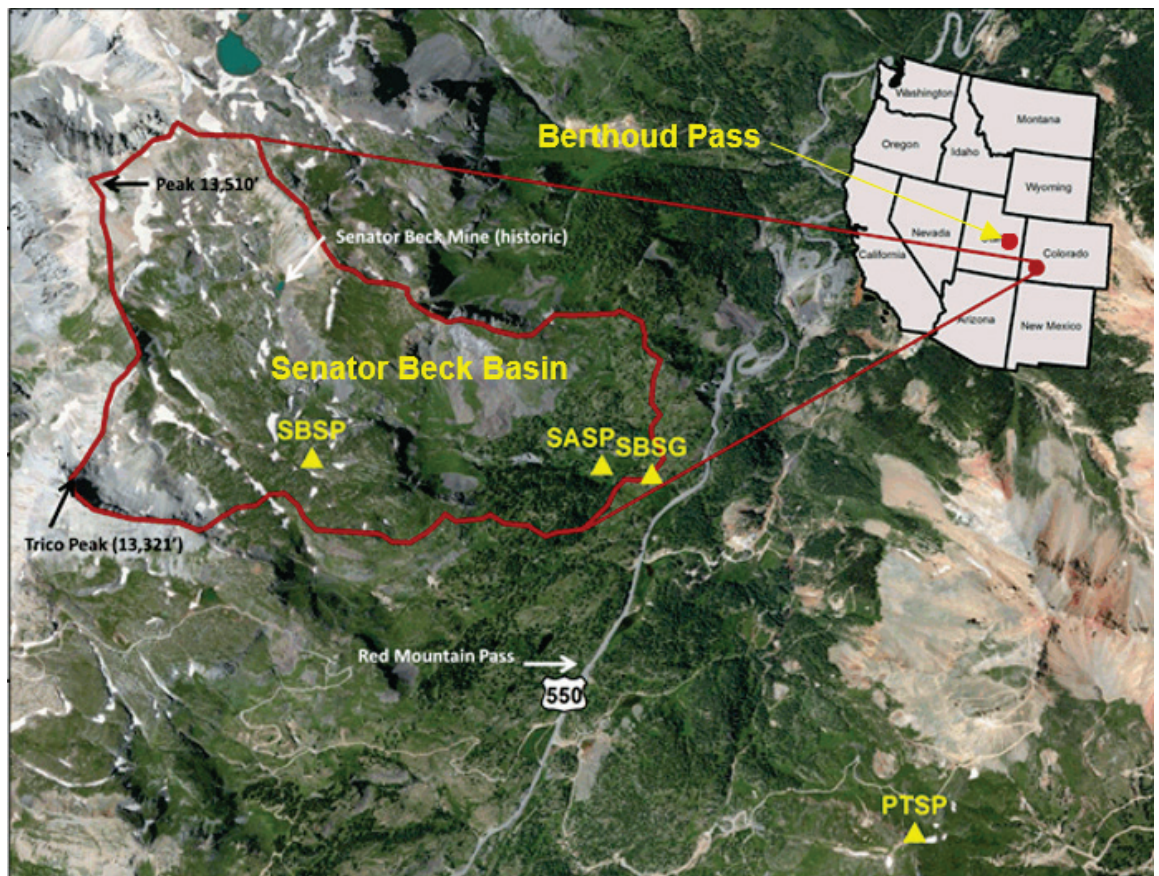


*Future Investment Fund*

## **Microscale Dynamics between Dust and Microorganisms in Alpine Snowpack**

Alison K. Thurston, Zoe R. Courville, Lauren B. Farnsworth,  
Ross Lieblappen, Shelby A. Rosten, John M. Fegyveresi,  
Stacey J. Doherty, Robert M. Jones, and Robyn A. Barbato

March 2021



**The U.S. Army Engineer Research and Development Center (ERDC)** solves the nation's toughest engineering and environmental challenges. ERDC develops innovative solutions in civil and military engineering, geospatial sciences, water resources, and environmental sciences for the Army, the Department of Defense, civilian agencies, and our nation's public good. Find out more at [www.erdclibrary.on.worldcat.org/discovery](http://www.erdclibrary.on.worldcat.org/discovery).

To search for other technical reports published by ERDC, visit the ERDC online library at [www.erdclibrary.on.worldcat.org/discovery](http://www.erdclibrary.on.worldcat.org/discovery).

# **Microscale Dynamics between Dust and Microorganisms in Alpine Snowpack**

Alison K. Thurston, Zoe R. Courville, Lauren B. Farnsworth, Ross Lieblappen, Shelby A. Rosten, John M. Fegyveresi, Stacey J. Doherty, Robert M. Jones, and Robyn A. Barbato

*U.S. Army Engineer Research and Development Center (ERDC)  
Cold Regions Research and Engineering Laboratory (CRREL)  
72 Lyme Road  
Hanover, NH 03755-1290*

Final Technical Report (TR)

Prepared for Headquarters, U.S. Army Corps of Engineers (HQUSACE)  
Washington, DC 20314-1000

Under 6.2 Geospatial Research and Engineering (GRE) Army Terrestrial-Environmental Modeling and Intelligence System Science Technology Objective–Research (ARTEMIS STO-R); 6.1 Geospatial Research and Engineering (GRE)

## **Abstract**

Dust particles carry microbial and chemical signatures from source regions to deposition regions. Dust and its occupying microorganisms are incorporated into, and can alter, snowpack physical properties including snow structure and resultant radiative and mechanical properties that in turn affect larger-scale properties, including surrounding hydrology and maneuverability. Microorganisms attached to deposited dust maintain genetic evidence of source substrates and can be potentially used as bio-sensors.

The objective of this study was to investigate the impact of dust-associated microbial deposition on snowpack and microstructure. As part of this effort, we characterized the microbial communities deposited through dust transport, examined dust provenance, and identified the microscale location and fate of dust within a changing snow matrix.

We found dust characteristics varied with deposition event and that dust particles were generally embedded in the snow grains, with a small fraction of the dust particles residing on the exterior of the snow matrix. Dust deposition appears to retard expected late season snow grain growth. Both bacteria and fungi were identified in the collected snow samples.

# Contents

<b>Abstract</b> .....	<b>ii</b>
<b>Figures and Tables</b> .....	<b>iv</b>
<b>Preface</b> .....	<b>vii</b>
<b>1 Introduction</b> .....	<b>1</b>
1.1 Background .....	1
1.1.1 Dust deposition and snow melt .....	1
1.1.2 Dust provenance at study site .....	2
1.1.3 Dust-associated microorganisms .....	2
1.2 Objectives .....	4
1.3 Approach .....	4
<b>2 Methods</b> .....	<b>6</b>
2.1 Sample Collection .....	6
2.2 Snow microstructure .....	7
2.3 Meteorology .....	8
2.3.2 Putney Study Plot (PTSP) – The Summit Station .....	8
2.3.3 Senator Beck Study Plot (SBSP) – The Alpine Station .....	9
2.3.4 Swamp Angel Study Plot (SASP) – The Sub-Alpine Station .....	10
2.3.5 Berthoud Pass Summit Station .....	12
2.4 Back trajectory modeling .....	12
2.5 Cell culturing .....	13
2.6 DNA sequencing .....	14
<b>3 Experiments and Results</b> .....	<b>16</b>
3.1 Snow microstructure .....	16
3.2 Meteorological station data analysis .....	20
3.3 Back trajectory modeling .....	23
3.4 Cell culturing .....	24
3.5 Microbial composition .....	24
<b>4 Discussion</b> .....	<b>28</b>
<b>References</b> .....	<b>30</b>
<b>Acronyms and Abbreviations</b> .....	<b>33</b>
<b>Appendix A: Meteorology of the Senator Beck Basin</b> .....	<b>35</b>
<b>Report Documentation Page (SF 298)</b> .....	<b>48</b>

# Figures and Tables

## Figures

1	CSAS Map indicating sample site locations in Colorado. The Senator Beck Study Plot (SBSP), Swamp Angel Study Site (SASP), Senator Beck Stream Gauge (SBSG) and Putney Study Plot (PTSP) are indicated by yellow triangles within the Senator Beck Basin (SBB). Samples were collected at the SASP and Berthoud Pass.....	5
2	Putney Study Plot Station (PTSP).....	9
3	Senator Beck Study Plot Station (SBSP).....	10
4	Swamp Angel Study Plot Station (SASP).....	11
5	Micro-CT segmentation of dust in representative snow samples. The gray material is the snow matrix. Orange specks are dust particles located on the snow-pore interface.....	16
6	NIR image of snow pit SC5 with merged dust layer at 11 cm depth.....	17
7	Microstructural characterization of dust particles in snow samples SC1, SC4, and SC5. The top panels show the number of particles per cubic millimeter and average thickness of the particles for all five samples containing noticeable quantities of dust. The bottom panels show the S/V ratio and degree of anisotropy .....	17
8	Surface to volume ratios of the snow phase in SC1 (merged layer from Berthoud Pass), SC4 (as-deposited layer from SASP, collected immediately following event D4), and SC5 (merged layer from SASP) compared to clean snow .....	19
9	3D micro-CT image of dust particles located on the surface of snow grains.....	19
10	Dust surface area exposed to air rather relative to embedded in the snow grain for samples SC1, SC4, and SC5 .....	20
11	Wind data from PTSP station. Highlighted areas indicate the four depositional events noted in Tbl. 3. Wind speeds are shown as 1-hour average resultant wind speeds ( $\text{m s}^{-1}$ ) .....	21
12	Wind data from SBSP station. Highlighted areas indicate the four depositional events noted in Tbl. 3. Wind speeds are shown as a 1-hour average resultant wind speeds ( $\text{m s}^{-1}$ ) .....	21
13	Wind data from SASP station collected during spring 2017. Highlighted areas indicate the four depositional events noted in Tbl. 3. Wind speeds are shown as a 1-hour average resultant wind speeds ( $\text{m s}^{-1}$ ).....	22
14	Wind data from Berthoud Pass METAR station collected during spring 2017. Wind speeds are shown as a 1-hour average resultant wind speeds ( $\text{m s}^{-1}$ ). Highlighted areas indicate possible dust deposition events .....	22
15	HYSPLIT simulation results for dust events D1-D4 (top left to bottom right) at SASP .....	23
16	HYSPLIT frequency backward trajectories for the dust deposition events for Berthoud Pass, Colorado.....	24
17	Dust-associated microbial colonies after incubation at 4 °C (left) and 25 °C (right) for dust from sample SC4. The left column indicates media type, and the bottom row indicates temperature.....	25

## Figures

18	PCoA plot of bacterial communities at the phylum level. Each point represents DNA sequences collected from a sample from the location .....	26
19	Relative abundance of bacteria at the phylum level. Each bar represents one replicate of the sample .....	27
A-1	PTSP wind data for event D1. Average wind speed and cardinal direction were 17.87 m s <sup>-1</sup> and 218 degrees, respectively.....	35
A-2	PTSP wind data for event D2. Average wind speed and cardinal direction were 11.68 m s <sup>-1</sup> and 203 degrees, respectively.....	36
A-3	PTSP wind data for event D3. Average wind speed and cardinal direction were 10.66 m s <sup>-1</sup> and 178 degrees, respectively .....	36
A-4	PTSP wind data for event D4. Average wind speed and cardinal direction were 13.40 m s <sup>-1</sup> and 231 degrees, respectively.....	37
A-5	SBSP wind data for event D1. Average wind speed and cardinal direction were 10.38 m s <sup>-1</sup> and 266 degrees, respectively.....	38
A-6	SBSP wind data for event D2. Average wind speed and cardinal direction were 5.45 m s <sup>-1</sup> and 197 degrees, respectively.....	38
A-7	SBSP wind data for event D3. Average wind speed and cardinal direction were 5.61 m s <sup>-1</sup> and 173 degrees, respectively.....	39
A-8	SBSP wind data for event D4. Average wind speed and cardinal direction were 6.92 m s <sup>-1</sup> and 256 degrees, respectively .....	39
A-9	Data incorporating specific wind rose diagrams and wind speeds from the SBSP .....	40
A-10	SASP wind data for event D1. Average wind speed and cardinal direction were 3.08 m s <sup>-1</sup> and 246 degrees, respectively .....	41
A-11	SASP wind data for event D2. Average wind speed and cardinal direction were 1.21 m s <sup>-1</sup> and 255 degrees, respectively .....	41
A-12	SASP wind data for event D3. Average wind speed and cardinal direction were 0.88 m s <sup>-1</sup> and 247 degrees, respectively.....	42
A-13	SASP wind data for event D4. Average wind speed and cardinal direction were 2.55 m s <sup>-1</sup> and 253 degrees, respectively .....	42
A-14	Data from incorporating specific wind rose diagrams and wind speeds over time at SASP.....	43
A-15	NOAA HYSPLIT model, backward trajectories ending at 1800 Coordinated Universal Time (UTC) 06 Mar 17 (GDAS Meteorological Data).....	44
A-16	NOAA HYSPLIT model, backward trajectories ending at 2200 UTC 23 Mar 17 (GDAS Meteorological Data).....	45
A-17	NOAA HYSPLIT model, backward trajectories ending at 1400 UTC 31 Mar 17 (GDAS Meteorological Data).....	46
A-18	NOAA HYSPLIT model, backward trajectories ending at 1800 UTC 09 Mar 17 (GDAS Meteorological Data).....	47

## Tables

1	Senator Beck Basin Study Plot Stations.....	6
2	Samples collected in spring 2017 from Berthoud Pass (Fraser, Colorado), and the Swamp Angel Study Plot in SBB. Each sample consists of three replicate samples (A-C) from the same layer taken ~50 to 100 cm apart .....	7
3	Description of weather events in which a dust deposition event occurred and snow samples were collected. Compiled data are from the Center of Snow and Avalanche Studies .....	20
A-1	PTSP wind data .....	35
A-2	SBSP wind data.....	37
A-3	SASP wind data.....	40
A-4	Average wind direction for all event over each study plot station .....	43



## Preface

The work was performed for the Headquarters, U.S. Army Corps of Engineers (HQUSACE). Funding was provided by the U.S. Army Engineer Research and Development Center (ERDC) 6.2 Geospatial Research and Engineering (GRE) Army Terrestrial-Environmental Modeling and Intelligence System Science Technology Objective–Research (ARTEMIS STO-R) under Work Item T42 053HJo, Funding Account Number U4357509, “Dynamic Undisturbed Soils Testbed to Characterize Local Origins and Uncertainties of Dust (DUST-CLOUD),” and by ERDC 6.1 Geospatial Research and Engineering (GRE) under Work Item AT24 L6620L, Funding Account Number U4363500 “Dark materials in snow and their impacts on preferential sublimation and surface roughness.”

The work was performed by the Biogeochemical Sciences Branch (Dr. Justin Berman, Chief) and the Terrestrial and Cryospheric Sciences Branch (Dr. John Weatherly, Chief) of the Research and Engineering Division (Mr. David B. Ringelberg, Acting Chief), ERDC Cold Regions Research and Engineering Laboratory (CRREL). At the time of publication, the Deputy Director of ERDC-CRREL was Mr. David B. Ringelberg, and the Director was Dr. Joseph L. Corriveau.

COL Teresa A. Schlosser was Commander of ERDC, and Dr. David W. Pittman was the Director.

**THIS PAGE INTENTIONALLY LEFT BLANK**

# 1 Introduction

## 1.1 Background

### 1.1.1 Dust deposition and snow melt

Atmospheric processes transport materials across long distances. In fact, Uno et al. (2009) have shown that dust from the Taklimakan Desert in China has been transported one full circuit around the Earth. These microscopic particles include dust, volcanic ash and soot, microorganisms (i.e., bacteria, archaea, fungi, and viruses), chemicals, and minerals (Schuerger et al. 2018). Dust particles carry microbial and chemical signatures from dust source regions to deposition regions. The result of this phenomena has two possible applications relevant to U.S. Army operations. In the first, microorganisms become incorporated into, and can greatly alter, snowpack physical properties including snow structure, pore structure, and resulting radiative and mechanical properties. These processes affect the surrounding snow hydrology and maneuverability on a macro-scale and are important to consider for operations in snow-covered areas. Secondly, because it is very likely that the attached microorganisms maintain genetic evidence of substrates from their source area, they could provide improved capability to forensically identify adverse activities, e.g., training maneuvers, weapons development, deployment, and troop activities, in otherwise access-denied areas.

Dust material deposited on snow affects snow melt rates (Conway et al. 1996, Skiles et al. 2018). Dust particulates incorporated onto snow surfaces decrease surface albedo (reflective power) and increase the amount of energy absorbed through ultraviolet (UV) radiation causing accelerated snow melt. Microorganisms attached to the dust particles, once thought to die during atmospheric flight, have been shown to survive transport (Harding et al. 2011, Meola et al. 2015). When growth needs are met at the deposition site, these transported microbes can proliferate, causing dark organics to spread in spatial extent. In some instances, the microbes change color through various pigments they make. The optical properties associated with this activity changes the reflective properties of the surface snow.

### **1.1.2 Dust provenance at study site**

The Colorado Plateau is one of the largest dust producing regions in North America along with the Great Basin, and the Mojave and Sonoran deserts. Mountain snow cover of the Colorado River Basin has seen increased dust loading from the Colorado Plateau with increased disturbance, starting in the middle 19th century to present (Skiles et al. 2015, references therein). In general, dust is deposited on snow through wet or dry events. Wet deposition events are those in which the dust falls as precipitation during snow deposition events. Dry events occur when wind blows lofted dust and deposits the dust on top of the snowpack.

When dust is deposited at the snow surface, it accelerates snow melt directly, by darkening the snow surface and reducing the albedo; and indirectly by accelerating the growth of snow grains (Skiles et al. 2015). Previous studies have focused on impacts to the snow surface due to dust deposition in the Senator Beck Basin Study Area in the San Juan Mountains of southwest Colorado (Painter et al. 2007, Lawrence et al. 2010, Painter et al. 2012, Skiles et al. 2015). Dust is transported from the southern Colorado Plateau and the Four Corners region by southwesterly winds (Skiles et al. 2015).

### **1.1.3 Dust-associated microorganisms**

Globally, an estimated 2 to 5 million metric tons of dust is lofted per year (Perkins 2001), providing a significantly large substrate for the transport of dust-associated microorganisms. Recent work has begun to examine biomass associated with dust particulates. Previously, microorganisms associated with aerosolized dust were thought to be killed due to exposure to UV radiation during flight. This view has changed as evidence mounts regarding the attachment and growth of microorganisms to dust particulates when all basic survival needs are met (Meola et al. 2015; Schuerger et al. 2018). Aerosolized dust particulate has been accepted as a major source of microbial distribution, particularly to remote regions (Harding et al. 2011). Dust-associated microorganisms are a potential health and ecological concern (Weir-Brush et al. 2004, Comrie et al. 2005, Weil et al. 2017). The transport of isolated bacteria with no substrate is limited, with deposition distances less than 1 km (Kellogg and Griffin 2006); the same bacteria attached to a dust particle can be deposited anywhere in the world. For instance, microorganisms originating from the Saharan Desert have been found in the Caribbean and in the European Alps (Kellogg and Griffin 2006, Meola et al. 2015).

Since dust is deposited in regions with high volumes of snowpack, microbes attached to these particles are as well. Recent work has established that microorganisms are capable of surviving in the extreme environment of snow and ice. For example, studies from the Canadian High Arctic, Iceland, Greenland, and European Alps have investigated the extent of snow and ice microbial biodiversity using molecular tools (Lutz et al. 2015, Harding et al. 2011, Lutz et al. 2014, Meola et al. 2015). A study on the Mittivakkat Glacier in Greenland during the melt season found both temporal and spatial differences in the glacial microbial communities with observations including biofilms at snow-ice interfaces, green algal blooms, red algal blooms, and cryoconite holes dispersed along the glacier (Lutz et al. 2014). Additionally, they found albedo was reduced from 75% (clean snow) to as low as 20% (cryoconite holes with high volumes of microorganisms), depending on the extent of microbial growth and presence of dust particulates, providing compelling results to incorporate microbes in albedo models to forecast the extent of melt.

How geographically diverse dust-associated microbial populations are, is a pressing question in the field (Kellogg and Griffin 2006, Grantham et al. 2015). Primary producers (i.e., autotrophs) found in snow and ice are much more similar across global glacial regions than heterotrophic bacterial communities (Anesio et al. 2017). However, limitations due to molecular markers for eukaryotic organisms may contribute to the lack of reported diversity (Anesio et al. 2017). Dust deposited on snow can be from local, regional or global sources. Therefore, it is possible that a small subset of microorganisms have adapted to the snow environment and are dispersed globally. Alternatively, dust origin may have more influence on the microbial communities and instead the microbial communities exhibit similar functions/processes that allow for adaptation to snow environments (Kellogg and Griffin 2006). Comparing the dust collected during dust deposition events to possible dust origins will aid in answering this question. For example, it is predicted that a substantial amount of the dust deposited in the San Juan Mountains comes from Mojave Desert and the Colorado Plateau (Lawrence et al. 2010). The mechanisms responsible for microbial adaptability to the conditions experienced in the desert environment, such as sporulation and pigment production, has been suggested to also allow for adaptability to snow environments (Meola et al. 2015). Dust-associated microorganisms deposited on snow via dust particles may have different metabolic requirements (Anesio et al. 2017), pigmentation pro-

duction (Lutz et al. 2014, 2015), and growth rates when compared to native snow and ice microbiota. These factors likely affect snow melt because their processes and production of pigments could enhance the absorption of heat on the ice or snow surface.

## 1.2 Objectives

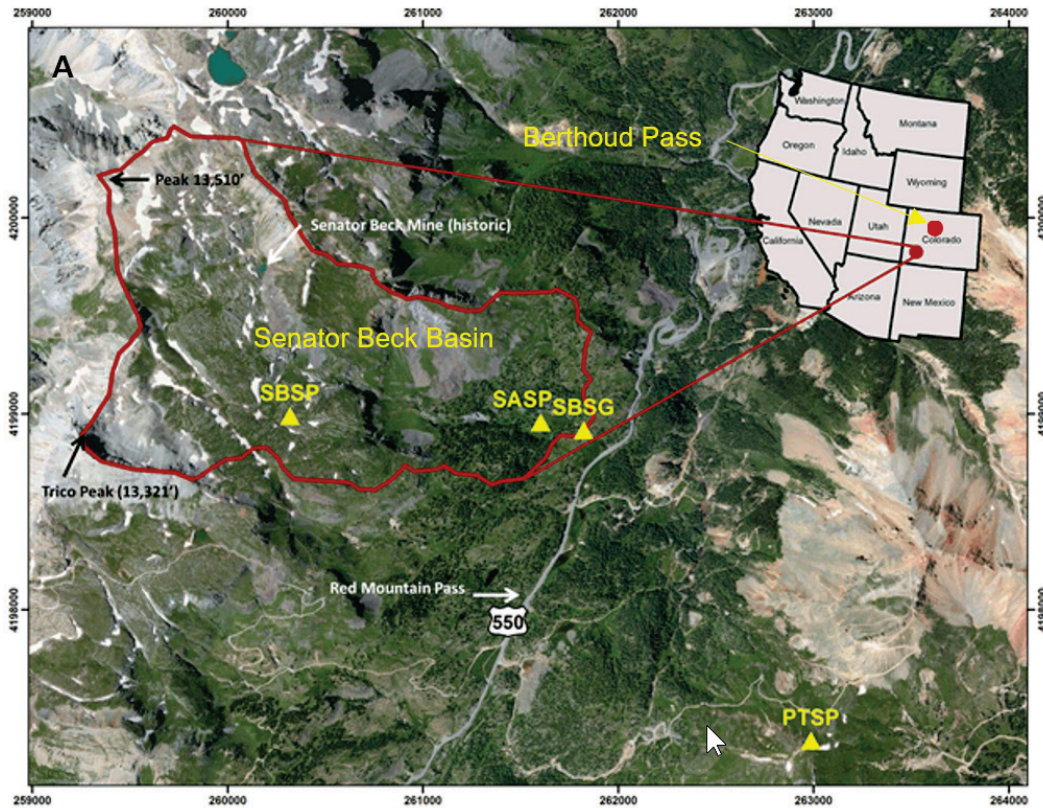
The focus of this study was to better understand the association between dust, microbes, and snow upon deposition and during melt at the onset of the spring season. We studied the effect that the deposited microbial communities may have on the snow matrix through altered localized, preferential radiative properties at the deposition site and by the microscale quantification of the dust location within the snow matrix during the melt season. Our final objective was to determine whether the microbial signature from a single dust event was still detectable once the dust layers mixed in the snowpack.

## 1.3 Approach

We used a multidisciplinary approach to investigate the identity of dust-associated microorganisms and their influence on the snow matrix during the melt season including microstructural analysis of dust and snow via micro-computed tomography (micro-CT), meteorology analysis, and microbial investigation including cell culturing and DNA sequencing.

Alpine snow samples were aseptically collected in collaboration with the Center for Snow and Avalanche Studies (CSAS) during multiple dust events in the late winter and early spring of 2017 for microbial studies. Coincident snow samples for microstructural analysis were collected for micro-CT investigations. The samples were collected from two different locations: the Berthoud Pass Colorado Dust-on-Snow (CODOS) site near Fraser, CO and Swamp Angel Study Plot (SASP) in Senator Beck Basin near Silverton, CO (Figure 1).

Figure 1. CSAS Map indicating sample site locations in Colorado. The Senator Beck Study Plot (SBSP), Swamp Angel Study Site (SASP), Senator Beck Stream Gauge (SBSG) and Putney Study Plot (PTSP) are indicated by yellow triangles within the Senator Beck Basin (SBB). Samples were collected at the SASP and Berthoud Pass.



Source: <http://snowstudies.org/sbbsa1.html>

Dust output and microbial community composition were measured from the snow samples; coincident snow microstructural analysis and the meteorology of the dust deposition events were examined to determine potential impacts to the snow structure and to determine the dust source location. We collected snow samples both immediately following dust deposition events as well as in the intervening months after deposition to examine subsequent post-depositional processes. We sought to discern the aggregated effect of multiple dust deposition events on the microbial communities.

## 2 Methods

For this study, both abiotic and biotic factors were investigated. Micro-CT scans were used to investigate the location of the dust within the snowpack in terms of microstructural parameters (i.e., pore space and relative location of dust). Real-time meteorological measurements and backward trajectory modeling were used to approximate the source of the dust deposits at the study sites. Microbial investigation included cell culturing and DNA sequencing to determine general microbial composition.

### 2.1 Sample Collection

Samples were collected from two alpine locations in Colorado; Berthoud Pass in the central Rocky Mountains near Fraser, Colorado (39°47'52"N, 105°46'37"W, 3446 m asl) and the SASP, located in the Senator Beck Basin in the San Juan Mountains, near Silverton, Colorado (37°54'25"N, 107°42'40"W, 3371 m asl) (Figure 1 and Table 1). These sites are both flat, relatively open areas located within forested regions. For microbial characterization, approximately 3 L samples were collected aseptically from surface snow and in snow pits immediately following new dust events, as well as later in the season subsequent to dust deposition. Three replicate samples from each dust layer in the snow pack were collected at each site, denoted by A-C following the sample name in Table 2. Replicate samples were taken approximately 50 to 100 cm from each other.

For sample collection immediately following dust deposition events, surface samples from the top 5 cm of the snow pack were collected. Over the course of the late spring, individual dust deposition layers in the snow typically merge into single layers due to snow processes including melt, grain growth due to temperature gradients within the snowpack, and sublimation/condensation. In addition to the samples collected immediately after dust deposition events, we collected a snow sample of a buried, merged dust layer.

Table 1. Senator Beck Basin Study Plot Stations.

Automatic Weather Station Name/Plot	Latitude	Longitude	Altitude (m)	Notes
Putney Study Plot (PTSP)	37°53'32.39" N	-107°41'44.77" W	3756	Summit Station
Senator Beck Study Plot (SBSP)	37°54'24.78" N	-107°43'34.56" W	3714	Alpine Station
Swamp Angel Study Plot (SASP)	37°54'24.89" N	-107°42'40.76" W	3371	Sub-Alpine Station
Berthoud Pass Summit Site (BPSS)	39°48' N	-105°47' W	3446	Sub-Alpine Station



Table 2. Samples collected in spring 2017 from Berthoud Pass (Fraser, Colorado), and the Swamp Angel Study Plot in SBB. Each sample consists of three replicate samples (A-C) from the same layer taken ~50 to 100 cm apart.

Sample Name (A, B, C indicate replicate samples)	Study Site	Date Collected	Dust Event
SC1- A, B, C	Berthoud Pass	May 1, 2017	Merged dust layer from Mar 9, 2017
SC2- A, B, C	SASP	March 25, 2017	Dust Event 2 (D2)
SC3- A, B, C	SASP	April 1, 2017	Dust Event 3 (D3)
SC4- A, B, C	SASP	April 10, 2017	Dust Event 4 (D4)
SC5- A, B, C	SASP	April 29, 2017	Merged dust layer
SC6- A, B, C	SASP (30 m to S-C5)	April 29, 2017	Merged dust layer
SC7- A, B, C	SASP	March 11, 2017	Dust Event 1 (D1)

Coincident sampling for microstructural characterization from the same snow pits sampled for microbial characterization occurred, with profile measurements of snow temperature, stratigraphy (via traditional means as well as recorded in near infrared (NIR) photography), and density within the snow pits. Sample volumes of 20 cm x 15 cm x 10 cm were collected, shipped back to the lab while frozen, and sub-sampled for micro-CT scanning (volumes of 5 cm x 2 cm x 2 cm).

## 2.2 Snow microstructure

To determine the location of dust particles within the 3D snow matrix, we imaged snow samples using a Bruker Skyscan 1173 micro-CT scanner housed in a -10 °C cold room. We focused on samples collected during the late spring at the primary SASP study site (merged layers SC5 and SC6), samples collected immediately after a dust event 4 (D4) at SASP (sample SC4), and a sample from a merged dust layer from a pit at Berthoud Pass (sample SC1). Each sample was scanned with 40 kV X-rays at 200 mA and a nominal resolution of approximately 15  $\mu\text{m}$  as the sample was rotated 180° in 0.4° steps with an exposure time of 300-350 ms. X-rays were detected using a 5 megapixel (2240 x 2240) flat panel sensor using 2x2 binning, and projection radiographs were averaged over four frames. The resulting 1120 x 1120 radiographs were then reconstructed into 2-D grayscale horizontal slices using NRecon software (Bruker), which uses a modified Feldkamp cone-beam algorithm. Image reconstruction processing included sample-specific post alignment, Gaussian smoothing using a kernel size of 2, sample-specific ring artifact correction of dead pixels, beam hardening correction, and X-ray source thermal drift correction.

Grayscale images were segmented into three phases: air (lowest X-ray absorption), dust (highest X-ray absorption), and snow (intermediate X-ray absorption). Segmenting thresholds for each of the phases were determined by finding the local minimum between peaks on the histogram showing all grayscale values. Dust and snow microstructural parameterizations were analyzed using the software package CTAn (Bruker's proprietary CT Analysis program). Microstructural parameters that we calculated using CTAn include the total porosity of the samples, the number of particles or objects of each phase, the surface-to-volume ratio (S/V) of each phase (which is inversely related to the grain size), and structure thickness (an estimate of particle/pore size).

## 2.3 Meteorology

We compiled meteorological data from three weather stations located at various elevations in Senator Beck Basin (SBB) near Silverton, Colorado, installed and maintained by CSAS. These stations include Putney Study Plot (PTSP), Senator Beck Basin Study Plot (SBSP), and SASP, which was our main sample collection area (Figure 1). Data captured at these stations includes ambient air temperature, humidity, wind direction, and wind speed. Data were recorded by Campbell Scientific CR10x data loggers, with measurements taken every 5 seconds and averaged each hour to generate 1-hour data, and once every 24 hours to generate a 24-hour summary. These measurements were used to evaluate wind direction and speed associated with a number of depositional events to better constrain the provenance of the deposited dust. Times reported are in Mountain Standard Time (ignoring Daylight Savings Time).

### 2.3.2 Putney Study Plot (PTSP) – The Summit Station

The CSAS's Putney Study Plot (PTSP) is located outside of SBB proper, approximately 1.5 km east-southeast of Red Mountain Pass on the ridge crest dividing the Mineral Creek and Cement Creek watersheds (Figure 1). Because of its high location on a small summit at 3756 m, PTSP monitors atmospheric conditions that are comparatively uninfluenced by local terrain (Figure 2). These measurements are considered representative of the general wind conditions in the Red Mountain Pass and SBB vicinity, and of ambient air temperatures at that elevation. Wind speed and direction (RM Young Model 05103-5) are measured every 5 seconds at the top of the 9-meter tower; air temperature and humidity (Vaisala HMP35-C) are measured every 5 seconds at 3 m above the ground (and not closer to the

ground, to protect the sensor from blowing snow, pebbles, and other flying debris during strong wind events).

Figure 2. Putney Study Plot Station (PTSP).



Those 5-second measurements are averaged each hour to generate 1-hour data, and once every 24 hours, at midnight, to generate 24-hour summary data using a Campbell Scientific CR10x datalogger. Times reported are in Mountain Standard Time (ignoring Daylight Savings Time).

### **2.3.3 Senator Beck Study Plot (SBSP) – The Alpine Station**

SBSP is located at a level site near the center of the SBB Study Area at 3714 m, above treeline and in the alpine tundra (Figure 3). The SBSP consists of a single 10-meter tower, with an extensive array of instrumentation, and an adjoining 12 m x 36 m snow profile plot.

Figure 3. Senator Beck Study Plot Station (SBSP).



This very exposed location is subject to the full force of the alpine winds inside the Basin and, as such, measurements of wind speed and direction are reasonably representative of wind-affected snow cover formation and other processes within the Basin. SBSP is a poor location for measuring precipitation because of these dominant wind effects; a very large portion of snowfall would simply blow over the top of the precipitation collector. Because the site sits on a level bench near the middle of the SBB watershed, air temperature and humidity data from SBSP are minimally affected by the surrounding terrain and often present a smaller diurnal range than at the SASP. The terrain horizon to the east, south, and west is sufficiently low and open to enable meaningful measurements of incoming solar radiation and of outgoing long-wave radiation emitted from the snowpack surface.

Wind speed and direction are measured at SBSP at the top of the 9-meter tower to minimize the influence of the immediate terrain. Snowpack depth, also referred to as height-of-snow (HS), is measured, in meters, at the end of each hour by an ultrasonic distance sensor designed for monitoring HS. Air temperature (Celsius) and relative humidity (percent) are measured every 5 seconds at a fixed height on the tower. Incoming short- and long-wave radiation values are measured, in watts per square meter, every 5 seconds by individual sensors at the top of the tower.

#### **2.3.4 Swamp Angel Study Plot (SASP) – The Sub-Alpine Station**

The SASP is the primary study location for snow sampling. It is located below treeline in a sheltered, lower-elevation clearing (Figure 4) ringed by

sub-alpine forest toward the southern end of the SBB Study Area, at approximately 3371 m. This protected location provides an excellent setting for measuring precipitation and snowpack accumulation, where wind speeds are very low (winter hourly average is less than 1 m/s) and wind redistribution of snow cover is negligible. Correspondingly, it is a poor location for monitoring wind speeds or direction representative of the Red Mountain Pass vicinity. Because the site sits in a sheltered pocket at a relatively low elevation in the SBB watershed, air temperature and humidity data from SASP are strongly influenced by the surrounding terrain. Cool air draining from the upper basin often pools at the SASP site overnight, dropping overnight low temperatures well below those at the immediately adjoining terrain. Conversely, the absence of wind during the daylight hours often enables enhanced warming in still air, compared to the more exposed surrounding terrain.

Figure 4. Swamp Angel Study Plot Station (SASP).



SASP consists of a 6-meter pipe mast with an extensive array of instruments, a standalone precipitation gauge, and a surrounding 30 m x 30 m snow profile plot. The site is generally level, sloping 3 degrees ENE. Air temperature (Celsius) and relative humidity (percent) are measured every 5 seconds at a fixed height on the tower. In addition, we established an in-ground and snowpack temperature profile measurement station as part of this work.

### 2.3.5 Berthoud Pass Summit Station

The weather station at the Berthoud Pass Summit Site (BPSS) site is maintained by the U.S. Department of Agriculture Natural Resources Conservation Service as part of the National Water and Climate Center (NWCC). It is a sub-alpine site located below treeline, at approximately 3446 m elevation. Measurements are made hourly and include snow water equivalent (Sensotec 100-inch Transducer); air temperature (YSI extended range), snow depth, soil moisture (Hydraprobe Analog), soil temperature (Hydroprobe Analog), salinity, real dielectric constant, wind direction and speed, and solar radiation. Wind speed and direction are recorded at two alpine stations, one operated by the Colorado Avalanche Information Center (CAIC) located at 3615 m elevation, and the other a Meteorological Terminal Aviation Routine (METAR) weather station at 3807 m. Data are available near real-time on the NWCC website.\* The Berthoud Pass site, unlike the SBB site, is for the most part unmanned, and so the exact timing of dust events is generally unobserved and must be inferred based on meteorological data and snow pit analysis.

## 2.4 Back trajectory modeling

We ran several transport and dispersion simulations using the Hybrid Single Particle Lagrangian Integrated Trajectory (HYSPLIT) model provided by the National Oceanic and Atmospheric Administration (NOAA). The HYSPLIT model computes air parcel trajectories, and can be used to simulate transport, dispersion, chemical transformation, and deposition (Stein et al. 2015). The HYSPLIT model calculation method is a hybrid between a Lagrangian approach, using a moving frame of reference for the advection and diffusion calculations as the trajectories or air parcels move from their initial location, and an Eulerian approach, which uses a fixed three-dimensional grid as a frame of reference to compute pollutant air concentrations.

The HYSPLIT model is frequently used for back trajectory analysis to determine the origin of air masses and establish source-receptor relationships. A specific example of this would be to determine trajectories of windblown dust. The dispersion of a pollutant is calculated by assuming either puff or particle dispersion. In the puff model, puffs expand until they exceed the size of the meteorological grid cell (either horizontally or vertically) and then split into several new puffs, each with its share of the pollutant mass.

---

\* <https://wcc.sc.egov.usda.gov/nwcc/site?sitenum=335>

In the particle model, a fixed number of particles are advected about the model domain by the mean wind field and spread by a turbulent component. The model's default configuration, which we used in our analysis, assumes a 3-dimensional particle distribution (horizontal and vertical).

To determine the storm trajectories of the dust deposition events, we ran backward trajectory simulations for SBB using a grid-point statistical interpretation archive method known as the Global Data Assimilation System (GDAS), within HYSPLIT, operating at 1-degree resolution. We used the GDAS because it is a fairly robust, well-recognized meteorological method. We ran the "Trajectory Frequency" simulation option because it initiates a trajectory from a single location and height every 6 hours, sums the frequency that each trajectory passes over a grid cell, and then normalizes by either the total number of trajectories or endpoints. A trajectory may intersect a grid cell once or multiple times (with residence time options 1, 2, or 3). We used typical default settings of 120-plot resolution (dpi), zoom factor of 70, and an analyzing height of 500 meters (AGL). In addition, we ran our simulations with a trajectory frequency grid resolution of 1.0 degree, and with a starting interval of 3 hours. Even though most of our observations and samples are collected from SASP, for simplicity, we ran HYSPLIT for the Alpine station (Putney) only, due to its location at a high elevation site where it is more exposed, and where it experiences more consistent winds. This ultimately produced the best model results. For the Berthoud Pass site, we used the higher of the two weather stations (the METAR station at 3807 m).

## 2.5 Cell culturing

Traditional cell culturing techniques were used to assess the culturability of the microorganisms associated with the dust deposited on the snow samples. Because of the high probability of biomass associated with the high abundance of dust particles, a sample from dust event 4 (D4) at the SASP site (SC4) was selected for culturing. The snow sample was thawed overnight in the dark at 4 °C and the resulting water/particulate solution was used to inoculate agar plates containing different nutrients: nutrient agar (NA), trypticase soy agar (TSA), and Reasoner's agar (R2A). The first two media are higher nutrient and are used for general microbial growth. The latter is a low nutrient media specifically used to select for slow growing organisms in potable water. Approximately 40 ml of SC4 was melted for culture and 300 µl was plated on 1X concentration agar plates. The remaining snow melt was centrifuged and all but 3 ml of supernatant was removed.

This resulted in a ~10X concentrated sample, of which 300  $\mu$ l of was plated onto each agar. Plates were incubated in the dark at 25 °C and 4 °C.

## 2.6 DNA sequencing

To examine which microorganisms were associated with the dust deposited on snow, DNA was extracted using the MoBio PowerWater DNA Isolation Kit. Samples were prepared for DNA extraction in a -16 °C cold room using sterile technique to limit any contamination. Samples were thawed at 4 °C in the dark over a 3- to 5-day period and processed within 48 hours of melting. Due to the low dust concentration in the samples, the extraction protocol was modified as follows: melted samples were filtered onto two sterile filters (MoBio Water Filters, 0.22 $\mu$ m), and the resulting DNA was pooled after extraction. Care was taken to ensure the filter was not folded onto itself to maximize the exposure of dust to the beads in the bead tube. After filtration, samples were incubated at 65 °C for 10 minutes and subject to 30 minutes of vigorous vortexing (Luhung et al. 2015). DNA extraction controls were carried out in parallel with snow samples. Extraction controls consisted of 10 mL of sterile water undergoing the same protocol as the collected snow samples including the filtration step.

The V1-V2 region of the 16S rRNA gene for bacteria and archaea was sequenced using a ThermoFisher Ion Torrent Personal Genome Machine sequencer at the Microbiome Analysis Center (MBAC) at George Mason University based on the manufacturer's protocols. Bioinformatic analysis and visualization of the 16S rRNA amplicon data were conducted using the R (version 3.5.3, R Core Team 2018) packages `dada2`, `phyloseq`, and `ggplot2` (McMurdie and Holmes 2013, Callahan et al. 2016, Wickham 2016). In brief, Bam files converted to FastQ files were demultiplexed into individual sequencing files. Adapter removal and barcode trimming were done in R prior to running the forward reads through the `dada2` (version 1.10.1) pipeline. To remove low quality regions from the sequences, the first 10 base pairs (bp) were removed and sequences were trimmed to a consistent length (300 bp). Sequences were removed that had an expected error rate of 2 or higher, matched known PhiX contamination, or contained ambiguous bases. After dereplication, the error rates were estimated using `dada2` and then used to guide the construction of the amplicon sequence variant (ASV) table. Chimeric sequences were then removed using the pooled method in `dada2`. Taxonomy was assigned using RDP trainset 16 (DOI: 10.5281/zenodo.801828). In `phyloseq`, ASVs identified as chloroplast at the class level were removed. Additionally, the phylum *Fusobacteria* was removed because



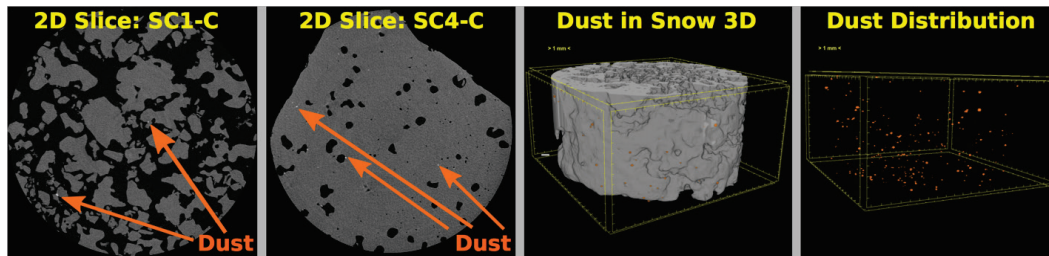
it had an ASV count of one, and the genus *Propionibacterium* was removed as it is a published human contaminant (Sheik et al. 2018). Taxa counts were converted to relative abundance and log transformed for normal distribution. To visualize differences in microbial taxonomy between sample types, Principal Coordinate Analysis (PCoA) dissimilarity plots were created using Bray-Curtis dissimilarity (Bray and Curtis 1957).

### 3 Experiments and Results

#### 3.1 Snow microstructure

The snow microstructural data obtained via micro-CT imaging was examined with the primary objective of determining where, within the snow matrix, the dust particles reside. Dust was most clearly identified on samples from the merged layer at Berthoud Pass (SC1-A, SC1-B and SC1-C), immediately after dust event D4 at SASP (SC4-A, SC4-B, SC4-C), and from the merged layer at SASP (SC5-A), collected during the late spring. After segmenting the snow, dust, and air phases (Figure 5), we quantified the microstructural parameters for each phase in two-dimensional (2D) cross-sections and in bulk three dimensions (3D).

Figure 5. Micro-CT segmentation of dust in representative snow samples. The gray material is the snow matrix. Orange specks are dust particles located on the snow-pore interface.



Dust layers were generally visible in snow pits excavated at the study sites, and can be readily seen in NIR images of the snow pit walls (Figure 6). The microstructural characteristics of the dust particles within the dust layer from the merged SC1-C sample, post-dust event samples SC4-A, SC4-B, SC4-C, and the merged SC5-A sample are shown in Figure 7. Snow pit SC5 had the highest concentration of dust, while snow pit SC1 had the lowest concentration. The structure thickness and S/V ratio of the dust particles was relatively similar for all samples, which indicates that the dust grain sizes are consistent between both the dust event SC4 (SASP as-deposited) and the merged layers SC1 (Berthoud Pass merged layer) and SC5 (SASP merged layer). Furthermore, this consistency suggests that dust grains remain relatively isolated from one another in the snow matrix and do not melt and group together. Finally, we calculated the degree of anisotropy, where 0 indicates perfectly isotropic (e.g., sphere) and 1 indicates the theoretical completely anisotropic. Although there was some anisotropy in the shape of the grains observed, the lack of a temporal trend suggests that the dust grains do not rotate or shift in a consistent manner over time.

Figure 6. NIR image of snow pit SC5 with merged dust layer at 11 cm depth.

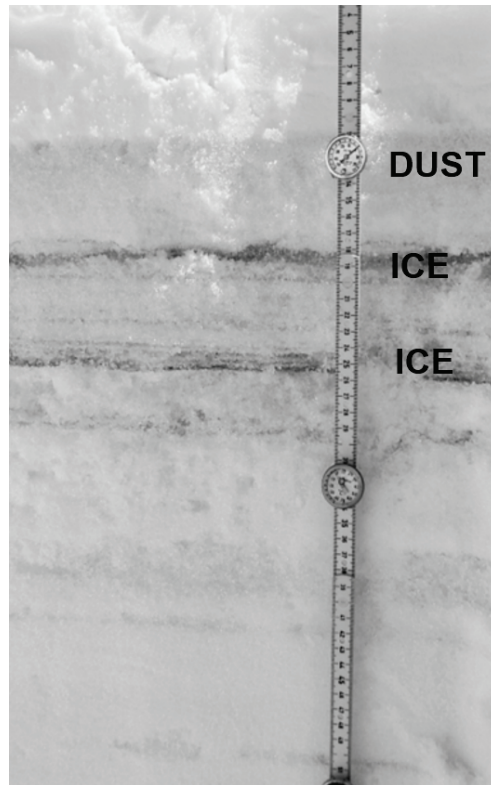
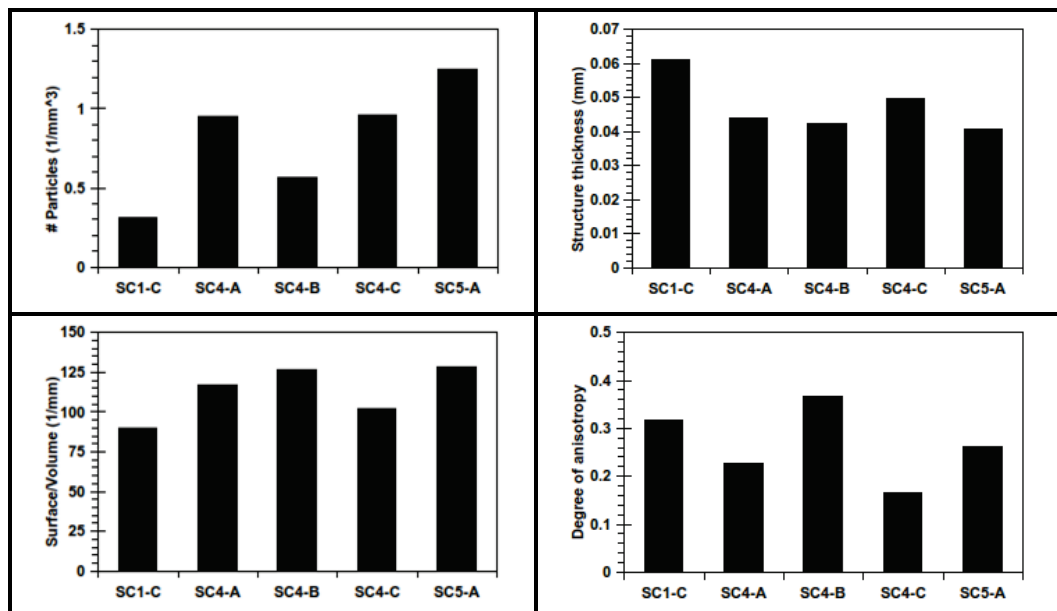


Figure 7. Microstructural characterization of dust particles in snow samples SC1, SC4, and SC5. The top panels show the number of particles per cubic millimeter and average thickness of the particles for all five samples containing noticeable quantities of dust. The bottom panels show the S/V ratio and degree of anisotropy.



We note that the number of dust particles per unit volume is an inherently noisy number due to the size of the dust particles. Since some of the dust particles were similar size to detector noise, we were not able to despeckle the image beyond a low-level Gaussian smoothing filter during image reconstruction. Therefore, the numerical value for dust particle density carries less validity than the relative number when comparing across samples. The Berthoud Pass sample (SC1) of merged dust layers clearly had a much lower amount of dust particles compared to the samples from SASP, most likely corresponding to the distance of the Berthoud Pass sample site to the dust deposition source. There is also a higher concentration of dust particles within the merged layer from SASP SC5 versus the as-deposited layer collected just after the dust event D4 from SASP SC4.

We found that dust and snow characteristics varied with site, particularly with snow porosity. The SC4 snow sample had very low porosity at 5% to 20%, which is nearly the value of ice, while SC1 and SC5 had porosities of 54% and 62%, respectively. Initial results suggest that grain growth processes dominated the S/V ratio of the snow particles (Figure 8), with the dust event with the highest concentration of dust particles (SC4) corresponding to the lowest S/V ratios. Snow samples that were collected immediately following deposition have low S/V ratio values, corresponding to larger snow grain sizes; while snow samples collected from the merged layers later in the season, have higher S/V ratio values, and corresponding smaller grain sizes. The merged dust layers, SC5 and SC1, sampled from the snow pack at the end of the season (April 29 and May 1, respectively) after longer residence time, had much higher S/V ratios than did the snow sampled immediately after the D4 dust deposition event, which corresponds to smaller grain sizes. This implies a lack of expected grain growth during the melt season. Typically, snow grains grow larger over time due to metamorphic processes related to temperature gradient driven movement of water vapor (Colbeck 1981). The small variability across replicate samples examined from the same layer (SC4-A through SC4-C) compared to layers merged after deposition (SC1 and SC5) shows consistency across a given dust layer.

Dust was generally observed to be located roughly on the exterior of snow grains (Figure 9). We next quantified how embedded the dust particles were in the snow to determine how much the dust resides on the surface versus how much it resides within the snow. We did this by dividing the surface area of the dust in contact with air by the total surface area of the dust.

Figure 8. Surface to volume ratios of the snow phase in SC1 (merged layer from Berthoud Pass), SC4 (as-deposited layer from SASP, collected immediately following event D4), and SC5 (merged layer from SASP) compared to clean snow.

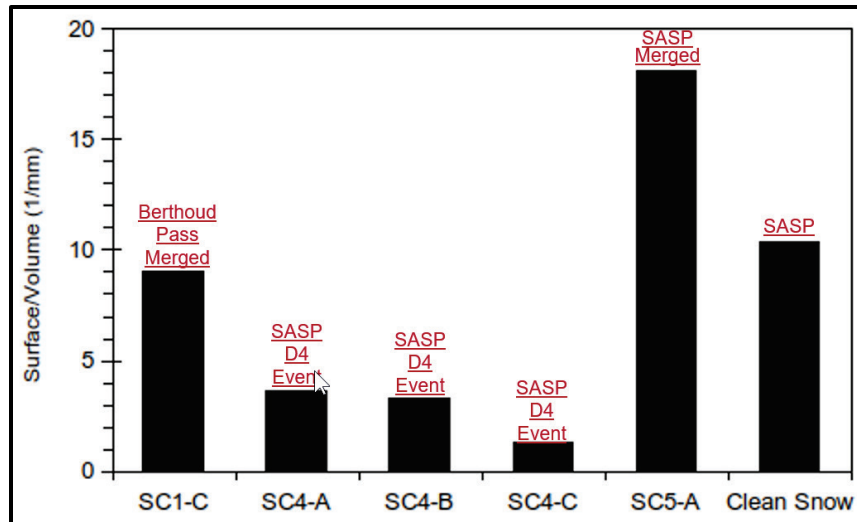
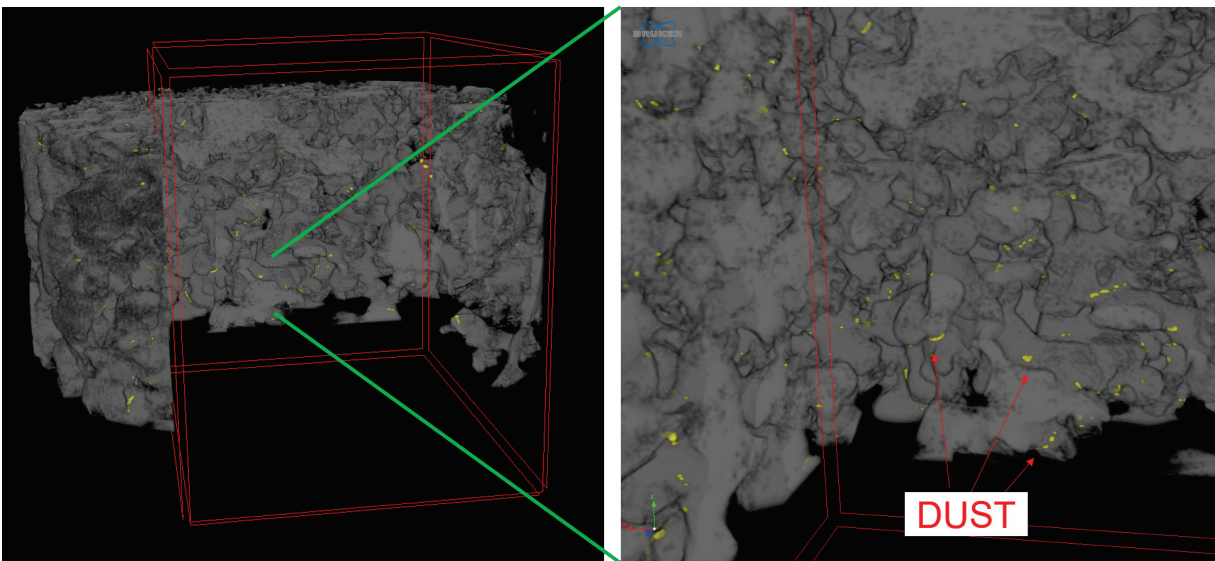
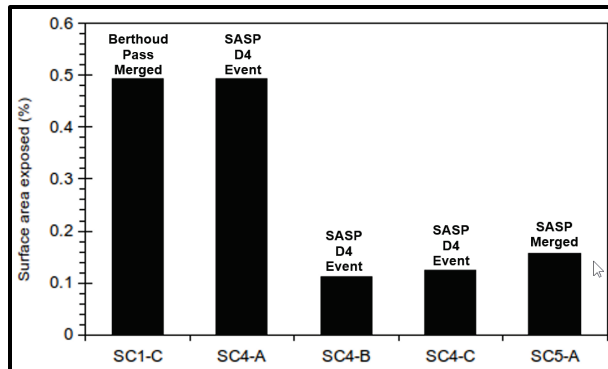


Figure 9. 3D micro-CT image of dust particles located on the surface of snow grains.



A dust particle completely embedded would have 0% exposure. Any value above 0% indicates the dust is on the surface of the snow grain. Higher values of exposure represent less embeddedness. We note that there is an upper limit as it is impossible for a dust particle to be 100% exposed (i.e., free floating). Figure 10 shows the percentage of surface area exposed for various deposition events. Dust tended to be less embedded and more on the surface for SC1-C and SC4-A, and more embedded for SC5, SC4-B, and SC4-C. Although these values are small, they are above 0, indicating that a small portion of dust particle surface area resides on the surface of the snow grain.

Figure 10. Dust surface area exposed to air rather relative to embedded in the snow grain for samples SC1, SC4, and SC5.



### 3.2 Meteorological station data analysis

In the spring of 2017, four separate depositional events occurred within the SBB area near Silverton, Colorado, as evidenced by visible dust layers on the snow surface (Table 3). For each depositional event, we examined the meteorological data captured by the three study plot stations (Table 1). Specifically, we evaluate wind direction and speed to better constrain the provenance of the deposited dust. Figures 11-13 show the average wind speed at each station during the spring of 2017. In each plot, the highlighted areas indicate the four depositional events noted in Table 3. Wind speeds are shown as 1-hour average resultant wind speeds ( $m s^{-1}$ ). Appendix A includes a more detailed meteorological analysis, including average cardinal wind direction.

In addition to studying the deposition events for the SBB, we examined the meteorology for dust events at the Berthoud Pass study site that occurred on March 6–9, 2017 and April 4–10, 2017 (Figure 14). This station is remote, so the dust deposition events were not directly observed, but had to be inferred from wind speed.

Table 3. Description of weather events in which a dust deposition event occurred and snow samples were collected. Compiled data are from the Center of Snow and Avalanche Studies.

Dust Event	Deposition Type	Average Wind Direction (degrees)	Average Wind Speed ( $m s^{-1}$ )	Peak Gust ( $m s^{-1}$ )	Start of Event	End of Event	Snow Sample
D1	Wet	218	18	36	3/5/17 12:00	3/6/17 10:00	SC7
D2	Wet	N/A*	N/A	N/A	3/23/17	N/A	SC2
D3	Wet	183	11	29	3/30/17 15:00	3/31/17 3:00	SC3
D4	Dry	228	13	27	4/8/17 13:00	4/9/17 9:00	SC4

\*Not Applicable (N/A)

Figure 11. Wind data from PTSP station. Highlighted areas indicate the four depositional events noted in Tbl. 3. Wind speeds are shown as 1-hour average resultant wind speeds ( $m s^{-1}$ ).

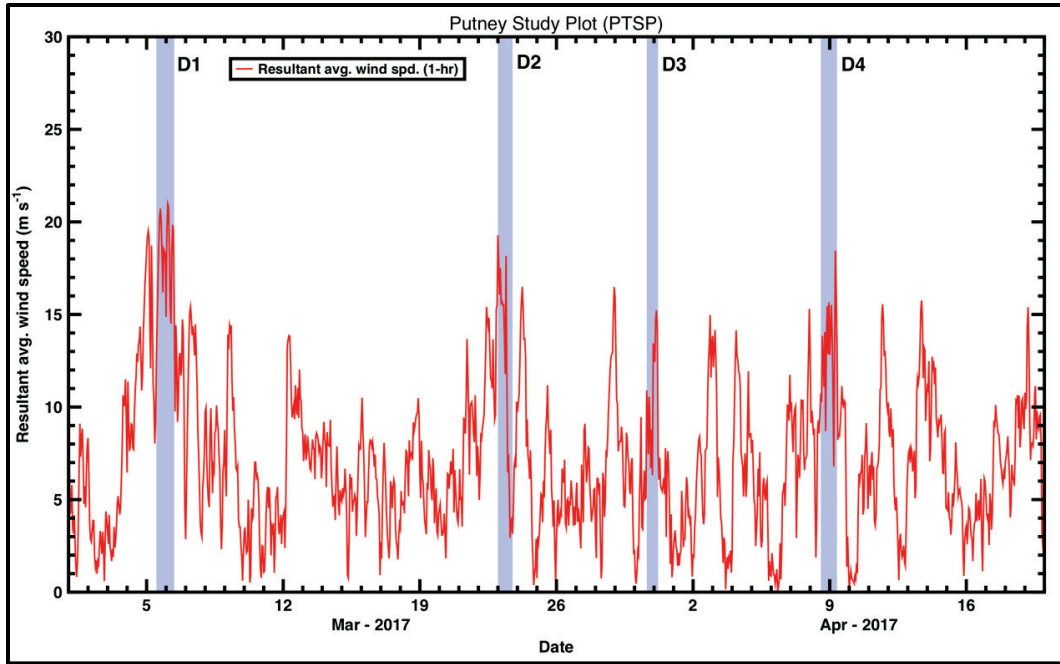


Figure 12. Wind data from SBSP station. Highlighted areas indicate the four depositional events noted in Tbl. 3. Wind speeds are shown as a 1-hour average resultant wind speeds ( $m s^{-1}$ ).

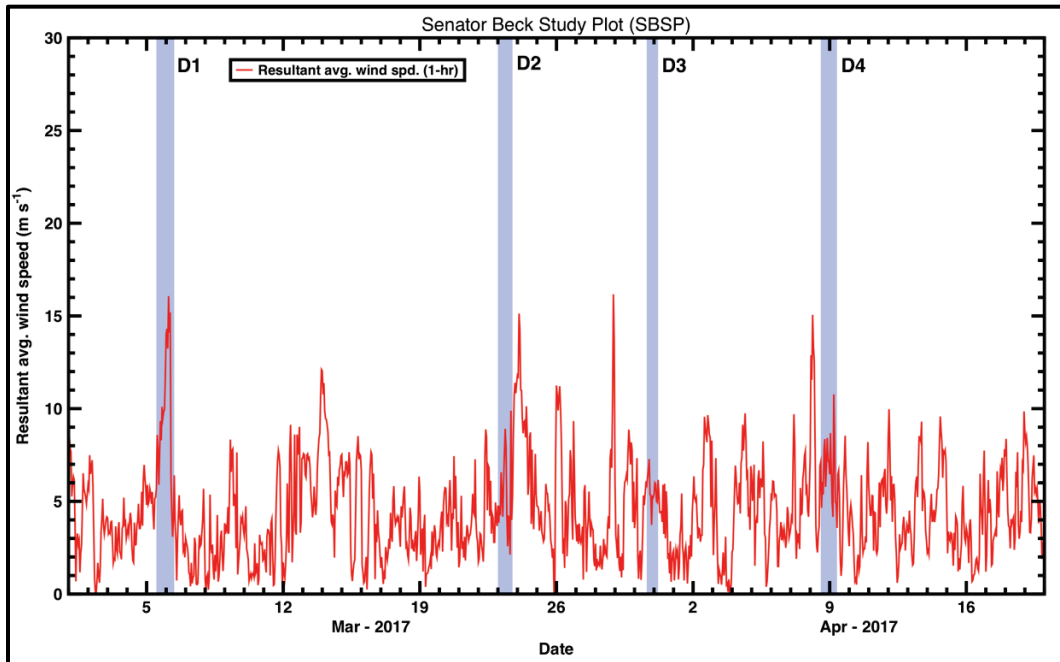


Figure 13. Wind data from SASP station collected during spring 2017. Highlighted areas indicate the four depositional events noted in Tbl. 3. Wind speeds are shown as a 1-hour average resultant wind speeds ( $m s^{-1}$ ).

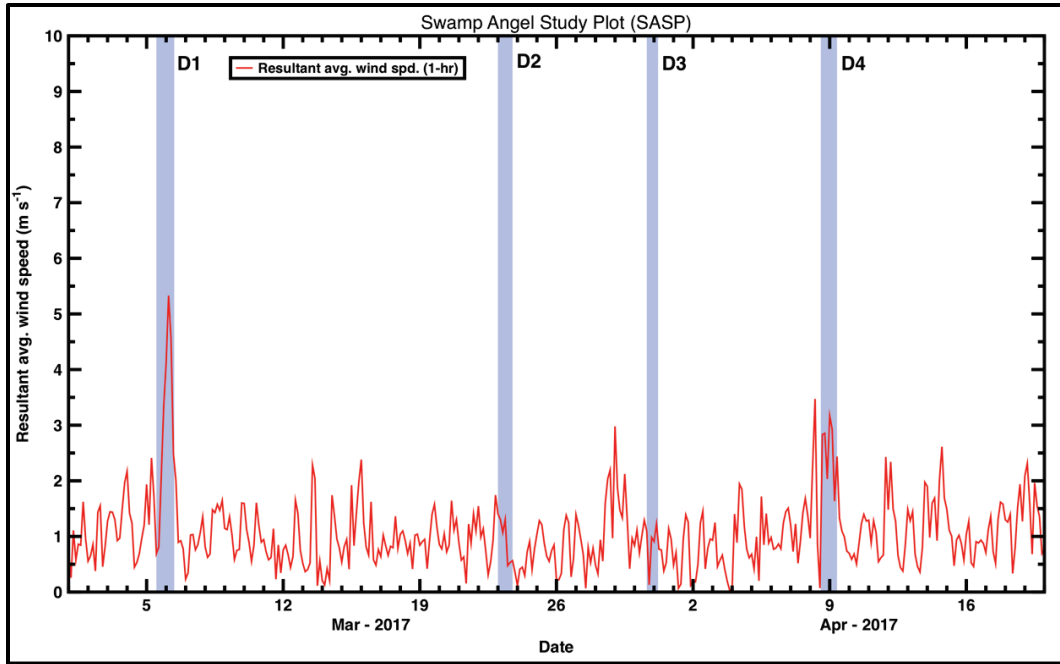
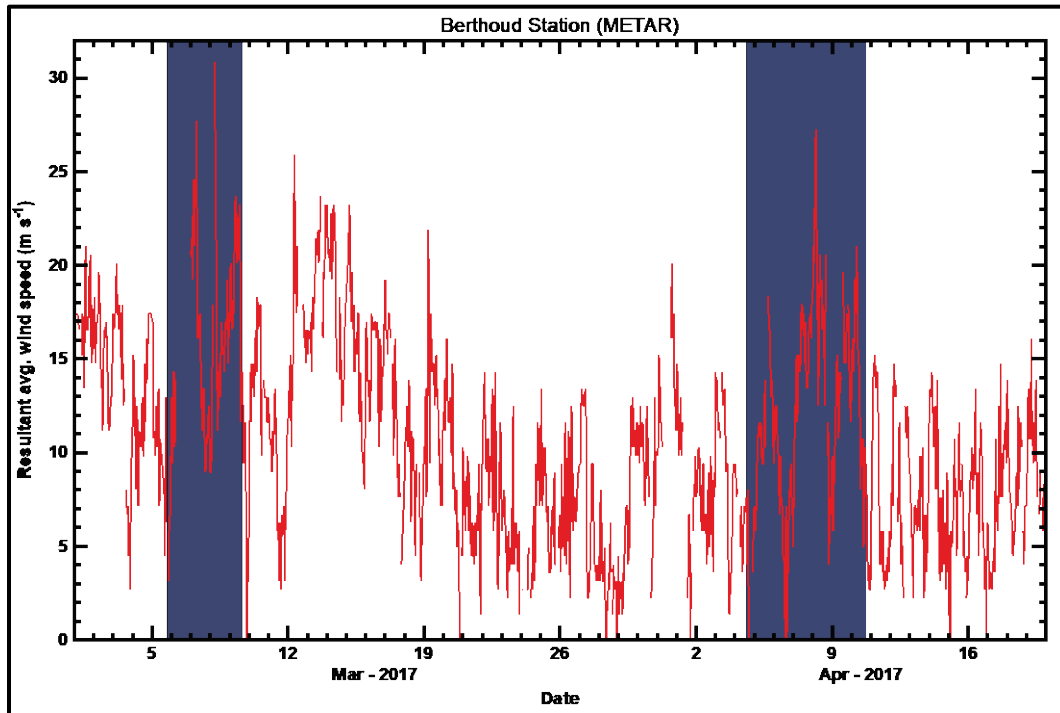


Figure 14. Wind data from Berthoud Pass METAR station collected during spring 2017. Wind speeds are shown as a 1-hour average resultant wind speeds ( $m s^{-1}$ ). Highlighted areas indicate possible dust deposition events.





### 3.3 Back trajectory modeling

The back trajectory results for SASP and Berthoud Pass (Figures 15 and 15, respectively) agree well with the average wind directions for each dust deposition event, D1-D4. (Appendix A includes detailed analysis of wind data.) In the majority of the events, the highest frequency for the trajectories, is found over the Four Corners region. For the case of dust event 2 (D2), the dust source is also a region east of the Four Corners area. Dust event 3 (D3) has the highest frequency of trajectories centered at SBB. This indicates a weak event, and that wind sources are difficult to identify accurately. Evidence for this is reflected in low peak wind gust for D3.

Figure 15. HYSPLIT simulation results for dust events D1-D4 (top left to bottom right) at SASP.

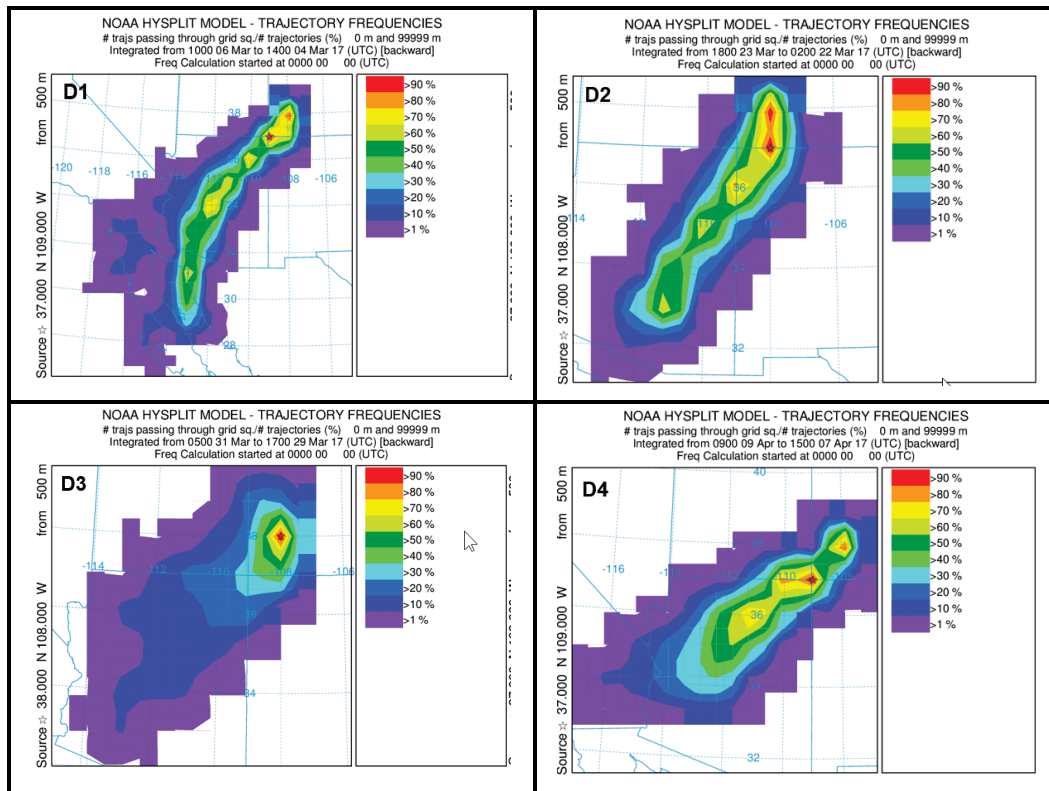
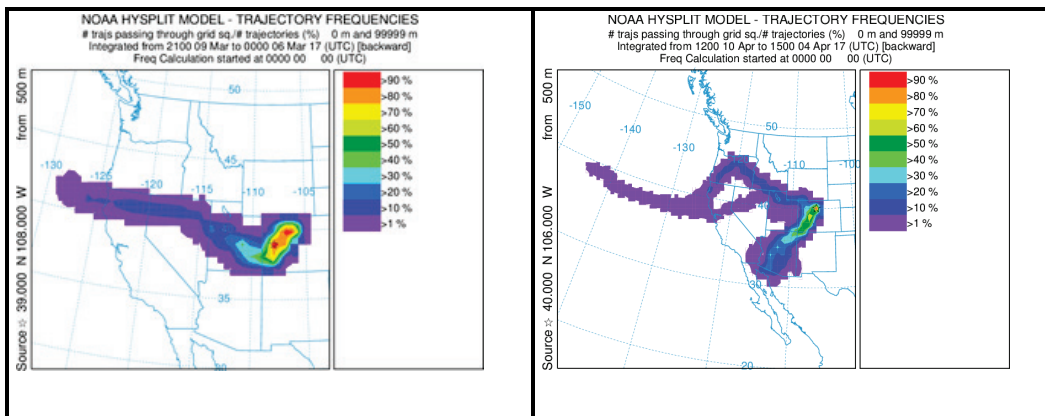


Figure 16. HYSPLIT frequency backward trajectories for the dust deposition events for Berthoud Pass, Colorado.



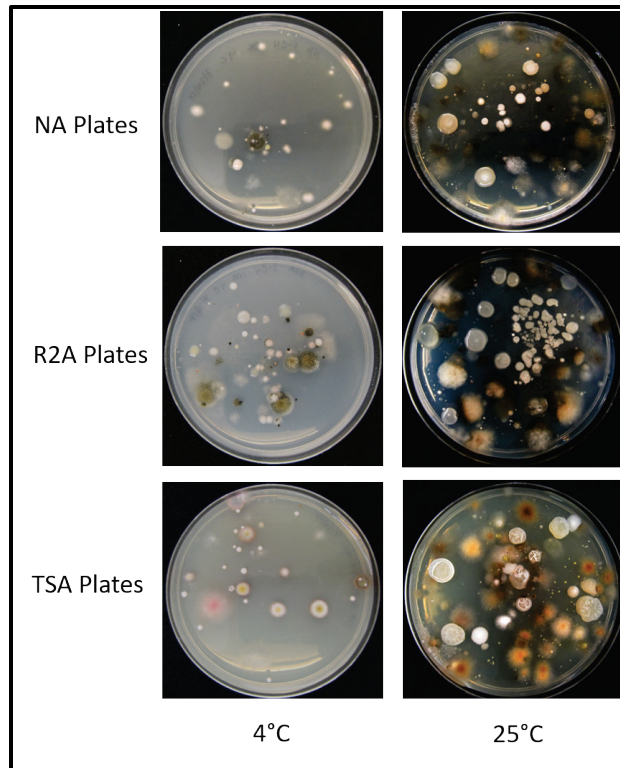
### 3.4 Cell culturing

Melted snow and dust particulate from a dust event 4 sample (SC4) were incubated on agar plates composed of different nutrient sources at two different temperatures. Bacterial and fungal colonies formed at 25 °C within a few days and formed at 4 °C within 30 days. The snow samples contained some culturable bacteria, but were dominated by culturable fungi, as evidenced by their morphology and the presence of hyphae (fuzzy appearance; Figure 17). The fungal source is not clear. Its origin may be from fungi associated with the dust particulate or the plant material observed in many of the samples. We also observed different organisms growing on different media inoculated at the same temperature, indicating heterogeneity in the sample and preference by the microbes for different growth substrates (Figure 17). As expected, fewer bacterial and fungal colonies grew at 4 °C because growth is typically slower at lower temperatures, unless the microbe is adapted to and prefers low temperatures. Under all conditions tested (temperature and nutrient source), we observed pigmented microorganisms on the plates inoculated with snow from dust event 4 (D4). For instance, the TSA plate incubated at 4 °C contained a bright pink colony, warranting further investigation into the pigmentation of these dusty snow bacterial communities and how they may accelerate melt.

### 3.5 Microbial composition

Our aim was to investigate whether there were differences in microbial community structure between sites and dust events. To assess these differences, we used DNA sequencing and ordination techniques. The PCoA plot accounted for 36.7% of the variation in the dataset (Figure 18).

Figure 17. Dust-associated microbial colonies after incubation at 4 °C (left) and 25 °C (right) for dust from sample SC4. The left column indicates media type, and the bottom row indicates temperature.

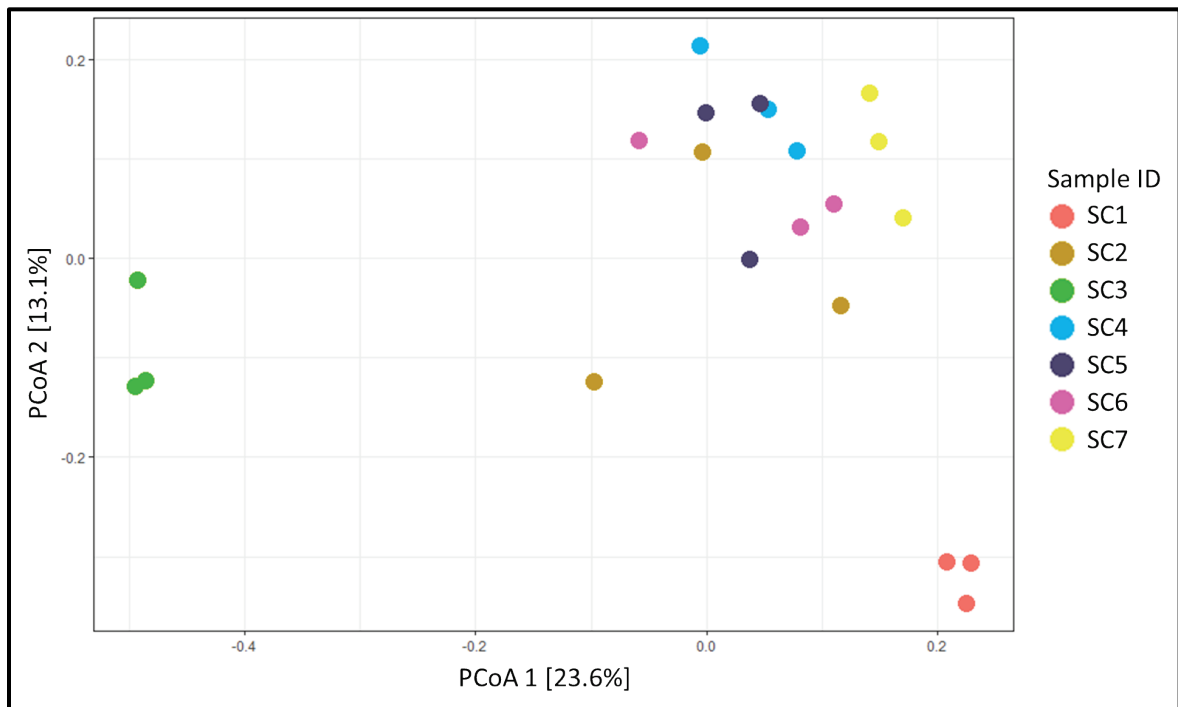


First, we assessed whether there were differences in microbial taxonomy between locations by comparing snow samples collected from Berthoud Pass (SC1) to snow samples collected from SASP (SC2 to SC7). The microbial communities from Berthoud Pass (SC1) clustered away from communities from SASP (SC2-SC7), indicating that the bacteria in the SC1 samples had a different composition from those in the SASP samples (Figure 18). Therefore, location is an important factor in the snow microbial community composition and should be considered when comparing snow samples collected from different sites.

Second, we examined differences in the community composition between dust samples collected at a single location to determine if dust deposition impacted microbial community structure. For this, we compared snow samples from SASP, which were SC2 to SC7 (Figure 18). Interestingly, samples from dust event 3 (SC3) clustered separately from the other SASP samples (Figure 18). These samples were collected from an individual dust event that occurred on March 30<sup>th</sup> and suggest that different dust events result in changes to microbial community structure. However, other dust events resulted in similar microbial communities. For instance, microbial

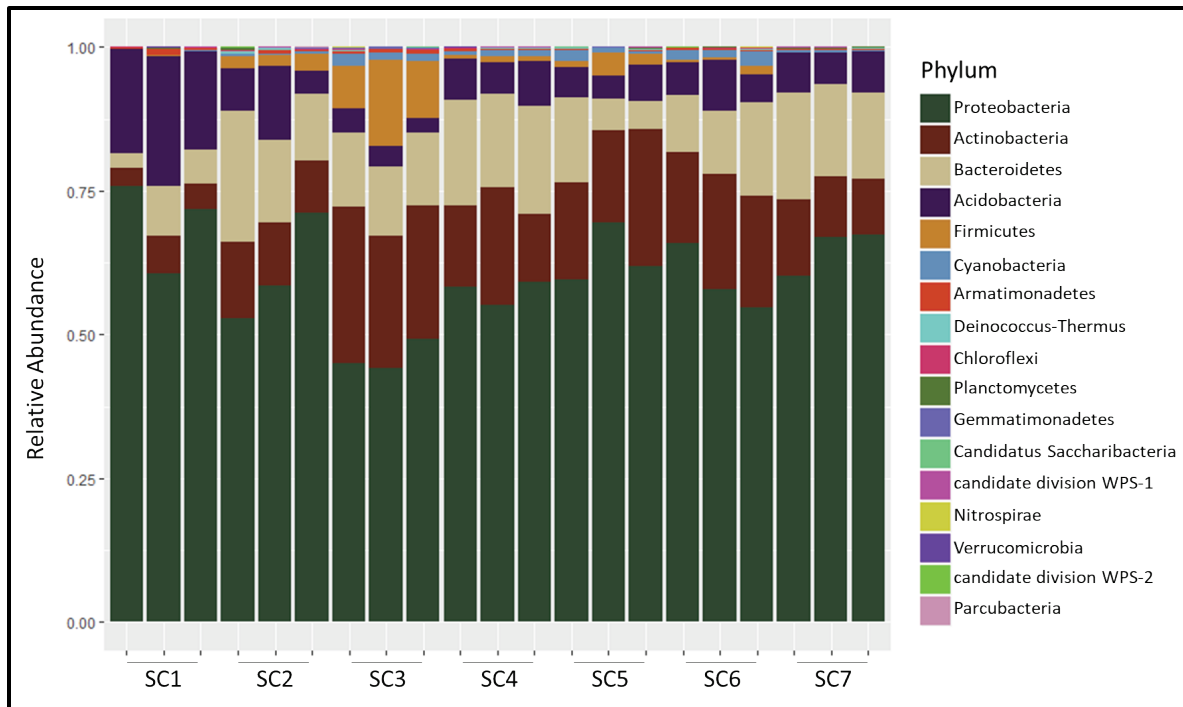
communities from dust event 1 (SC7) and dust event 4 (SC4), occurring on March 5<sup>th</sup> and April 8<sup>th</sup> respectively, clustered together and therefore harbored similar microbial taxa. Samples from dust event 2 (SC2) are more similar to dust event 1 (SC7) and dust event 4 (SC4) than dust event 3 (SC3); however the replicate samples from dust event 2 (SC2) do not form a tight cluster indicating there is greater heterogeneity within the collected samples (Figure 18). Also of note is that the two merged samples SC5 and SC6 contained microbial communities that are similar to the samples collected from the individual dust events (1, 2, and 4) with the exception of dust event 3 (Figure 18).

Figure 18. PCoA plot of bacterial communities at the phylum level. Each point represents DNA sequences collected from a sample from the location.



To elucidate which microbes were present in the samples, relative abundance was examined at the phylum level (Figure 19). Proteobacteria, Actinobacteria, Bacteroidetes, Acidobacteria, and Firmicutes were the most dominant phyla in all of the snow samples (Figure 19); together, these phyla comprise ~98% of the identified microbial community in the samples. Proteobacteria were the most abundant in every sample, ranging from approximately 44% to 76% of the entire community (Figure 19). The samples collected in Berthoud pass (SC1) had lower levels of Actinobacteria and higher levels of Acidobacteria compared to the SASP samples. Dust event 3 (SC3) consisted of lower levels of Proteobacteria, Acidobacteria and higher levels of Firmicutes compared to other samples.

Figure 19. Relative abundance of bacteria at the phylum level. Each bar represents one replicate of the sample.



## 4 Discussion

Our study provides some of the first analyses of coupled snowpack microbial and microstructural characteristics of deposited dust events and subsequent fate within the snowpack. Microstructural analysis of the dust within the snow matrix suggests that, for the case of late season when snow layers have merged, dust resides at the snow/pore interface and not the interior of the snow grains. We found that the dust particles embedded toward the outside of snow grains have a low percentage of surface area exposed to air. The placement of the particle within the snowpack could have important implications if microbial cells are using the dust particles as substrate or attachment.

Over time, it appears that the presence of dust retards expected grain growth that would normally be predicted due to temperature gradient-driven metamorphosis (Colbeck 1982). The merged dust layers contain a higher concentration of dust and have much higher S/V ratios, which correspond to smaller grain sizes (also smaller grain sizes compared to clean snow); this corresponds to a lack of expected grain growth during the melt season. Typically, snow grains grow larger over time due to metamorphic processes related to temperature gradient driven movement of water vapor. Smaller grains have a higher albedo, perhaps offsetting some of the darkening effect caused by the dust. Limited grain growth can also be caused by a lack of solar radiation; the combined impacts to grain growth will be examined in future work.

Meteorology and subsequent back trajectory modeling suggest that the dust for the particular dust events examined for the Senator Beck region originated in the southern Colorado Plateau, with the wind trajectory coming from the south-west (Figure 15). The source region for the Berthoud Pass area is less clear (Figure 16). Interestingly, dust event 3 was a weak wind event with the frequencies over the SBB area, which made it difficult to determine the source region for the event. This event also coincides with relatively low wind speeds and peak gusts. Snow samples collected from dust event 3 (SC3) were the most distinct and harbored the lowest levels of Proteobacteria but had the highest levels of Firmicutes (Figure 19). Perhaps it was a more local source that resulted in a unique microbial community. Future sample collection should include clean snow samples from SASP, soil samples from Red Mountain Pass (near SASP) prior to snow accumulation, and soil samples from the Four Corners Region to associate

source material with aeolian transport and deposition to distinguish between the native microbial community and the foreign, aeolian transported microbial community.

The presence of both bacteria and fungi demonstrate their survival in snow. At the phylum level, Proteobacteria, Actinobacteria, Bacteroidetes, Acidobacteria, and Firmicutes accounted for the majority of the detected bacteria in all samples (~98%). Interestingly, the abundance of Cyanobacteria was low in all samples, this deviates slightly from the notion of a core snow microbiome of Proteobacteria, Bacteroidetes, Firmicutes, and Cyanobacteria (Hell et al., 2013; Hauptmann et al. 2014; Wunderlin et al. 2016). Cyanobacteria have been found in other cryosphere environments such as glaciers in west Greenland (Uetake et al. 2010) and snow in the Canadian High Arctic (Harding et al. 2011) and the Sierra Nevada, California (Carey et al. 2016). Investigations of the proliferation of different organisms under select growth conditions from different source material contribute to an understanding of the mechanisms associated with both survival and growth. This mechanistic understanding would serve as input variables to sophisticated models assessing snow melt in alpine regions. Furthermore, the assessment of environmental factors affecting growth is critical to explain how microbial dust transport influences foreign environments and regional snow packs. Additionally, it serves as a way to characterize microorganisms that can survive deposition onto snow packs. Combining these data with specific microbial signatures could provide a robust tool to better understand the origin and fate of dust on snow.

## References

- Anesio, A. M., S. Lutz, N. A. Christmas, and L. G. Benning. 2017. "The Microbiome of Glaciers and Ice Sheets." *NPJ Biofilms and Microbiomes* 3(1):10.
- Bray, J. R., and J. T. Curtis. 1957. "An Ordination of the Upland Forest Communities of Southern Wisconsin." *Ecological Monographs* 27(4):325-49.  
doi:org/10.2307/1942268.
- Callahan, B. J., K. J. A. Sankaran, P. Mcmurdie Fukuyama, and S. P. Holmes. 2016. "Bioconductor Workflow for Microbiome Data Analysis: From Raw Reads to Community Analyses." *F1000 Research* 5:1492,  
doi:10.12688/f1000research.8986.2.
- Caporaso, J. G., J. Kuczynski, J. Stombaugh, K. Bittinger, F. D. Bushman, E. K. Costello, N. Fierer, A. G. Pena, J. K. Goodrich, J. I. Gordon, and G. A. Huttley. 2010. "QIIME Allows Analysis of High-Throughput Community Sequencing Data." *Nature Methods* 7(5):335.
- Carey, C. J., S. C. Hart, S. M. Aciego, C. S. Riebe, M. A. Blakowski, and E. L. Aronson. 2016. "Microbial Community Structure of Subalpine Snow in the Sierra Nevada, California." *Arctic, Antarctic, and Alpine Research* 48(4):685-701.
- Colbeck, S. 1982. "An Overview of Seasonal Snow Metamorphism." *Reviews of Geophysics and Space Physics* 20(1):45-61.
- Comrie, A. C. 2005. "Climate Factors Influencing Coccidioidomycosis Seasonality and Outbreaks." *Environmental Health Perspectives* 113(6):688.
- Conway, H., A. Gades, and C. F. Raymond. 1996. "Albedo of Dirty Snow during Conditions of Melt." *Water Resources Research* 32(6):1713-1718.
- DeSantis, Todd Z., Philip Hugenholtz, Neils Larsen, Mark Rojas, Eoin L. Brodie, Keith Keller, Thomas Huber, Daniel Dalevi, Ping Hu, and Gary L. Andersen. 2006. "Greengenes, A Chimera-Checked 16S rRNA Gene Database and Workbench Compatible with ARB." *Applied and Environmental Microbiology* 72(7):5069-5072.
- Edgar, Robert C. 2010. "Search and Clustering Orders of Magnitude Faster than BLAST." *Bioinformatics* 26(19):2460-2461.
- Grantham, N. S., B. J. Reich, K. Pacifici, E. B. Laber, H. L. Menninger, J. B. Henley, A. Barberán, J. W. Leff, N. Fierer, and R. R. Dunn. 2015. "Fungi Identify the Geographic Origin of Dust Samples." *PLoS One* 10(4):e0122605.  
doi:10.1371/journal.pone.0122605.
- Harding, T., A. D. Jungblut, C. Lovejoy, and W. F. Vincent. 2011. "Microbes in High Arctic Snow and Implications for the Cold Biosphere." *Applied and Environmental Microbiology* 77(10):3234-3243.



- Hauptmann, A. L., M. Stibal, J. Bælum, T. Sicheritz-Pontén, S. Brunak, J. S. Bowman, L. H. Hansen, C. S. Jacobsen, and N. Blom. 2014. "Bacterial Diversity in Snow on North Pole Ice Floes." *Extremophiles*. 18(6):945-951. doi:10.1007/s00792-014-0660-y.
- Hell, K., A. Edwards, J. Zarsky, S. M. Podmirseg, S. Girdwood, J. A. Pachebat, H. Insam, and B. Sattler. 2013. "The Dynamic Bacterial Communities of a Melting High Arctic Glacier Snowpack." *ISME J*. 7(9):1814-1826. doi:10.1038/ismej.2013.51.
- Kellogg, C. A., and D. W. Griffin. 2006. "Aerobiology and the Global Transport of Desert Dust." *Trends in Ecology & Evolution* 21(11):638-644.
- Lawrence, C. R., T. H. Painter, C. C. Landry, and J. C. Neff. 2010. "Contemporary Geochemical Composition and Flux of Aeolian Dust to the San Juan Mountains, Colorado, United States." *Journal of Geophysical Research: Biogeosciences* 115(G3). doi:10.1029/2009JG001077.
- Lozupone, Catherine, and Rob Knight. 2005. "UniFrac: A New Phylogenetic Method for Comparing Microbial Communities." *Applied and Environmental Microbiology* 71(12):8228-8235.
- Luhung, I., Y. Wu, C. K. Ng, D. Miller, B. Cao, and V. W. C. Chang. 2015. "Protocol Improvements for Low Concentration DNA-Based Bioaerosol Sampling and Analysis." *PloS One* 10(11):e0141158.
- Lutz, S., A. M. Anesio, A. Edwards, and L. G. Benning. 2015. "Microbial Diversity on Icelandic Glaciers and Ice Caps." *Frontiers in Microbiology* 6:307. doi:10.3389/fmicb.2015.00307.
- Lutz, S., A. M. Anesio, S. E. Jorge Villar, and L. G. Benning. 2014. "Variations of Algal Communities Cause Darkening of a Greenland Glacier." *FEMS Microbiology Ecology* 89(2):402-414. doi:10.1111/1574-6941.12351.
- McMurdie, P. J., and S. Holmes. 2013. "phyloseq: An R Package for Reproducible Interactive Analysis and Graphics of Microbiome Census Data." *PLoS ONE* 8(4):e61217. doi: 10.1371/journal.pone.0061217.
- Meola, M., A. Lazzaro, and J. Zeyer. 2015. "Bacterial Composition and Survival on Sahara Dust Particles Transported to the European Alps." *Frontiers in Microbiology* 6:1454. doi:10.3389/fmicb.2015.01454.
- Painter, T. H., S. M. Skiles, J. S. Deems, A. C. Bryant, and C. C. Landry. 2012. "Dust Radiative Forcing in Snow of the Upper Colorado River Basin: 1. A 6 Year Record of Energy Balance, Radiation, and Dust Concentrations." *Water Resources Research* 48(7).
- Painter, T. H., A. P. Barrett, C. C. Landry, J. C. Neff, M. P. Cassidy, C. R. Lawrence, K. E. McBride, and G. L. Farmer. 2007. "Impact of Disturbed Desert Soils on Duration of Mountain Snow Cover." *Geophysical Research Letters* 34(12).
- Perkins, S. 2001. "Dust, the Thermostat How Tiny Airborne Particles Manipulate Global Climate." *Science News* 160(13):200-2002.

- Price, M. N., P. S. Dehal, and A. P. Arkin. 2010. "FastTree 2—Approximately Maximum-Likelihood Trees for Large Alignments." *PLoS One* 5(3):e9490.
- R Core Team. 2018. *R: A Language Environment for Statistical Computing*. Vienna, Austria: R Foundation for Statistical Computing. [www.R-project.org](http://www.R-project.org).
- Schuerger, A. C., D. J. Smith, D. W. Griffin, D. A. Jaffe, B. Wawrik, S. M. Burrows, B. C. Christner, C. Gonzalez-Martin, E. K. Lipp, D. G. Schmale III, and H. Yu. 2018. "Science Questions and Knowledge Gaps to Study Microbial Transport and Survival in Asian and African Dust Plumes Reaching North America." *Aerobiologia* 34(4):425-435.
- Sheik, C. S., B. K. Reese, K. I. Twing, J. B. Sylvan, S. L. Grim, M. O. Schrenk, M. L. Sogin, and F. S. Colwell. 2018. "Identification and Removal of Contaminant Sequences From Ribosomal Gene Databases: Lessons From the Census of Deep Life." *Frontiers in Microbiology*. 9:840. doi:10.3389/fmicb.2018.00840.
- Skiles, S. M., T. H. Painter, J. Belnap, L. Holland, R. L. Reynolds, H. L. Goldstein, and J. Lin. 2015. "Regional Variability in Dust-on-Snow Processes and Impacts in the Upper Colorado River Basin." *Hydrological Processes* 29(26):5397-5413.
- Skiles, S. M., M. Flanner, J. M. Cook, M. Dumont, and T. H. Painter. 2018. "Radiative Forcing by Light-Absorbing Particles in Snow." *Nature Climate Change* 8:964-971.
- Stein, A. F., R. R. Draxler, G. D. Rolph, B. J. B. Stunder, M. D. Cohen, and F. Ngan. 2015. "NOAA's HYSPLIT Atmospheric Transport and Dispersion Modeling System." *Bulletin of the American Meteorological Society* 96:2059–2077.
- Uetake, J., T. Naganuma, M. B. Hebsgaard, H. Kanda, and S. Kohshima. 2010. "Communities of Algae and Cyanobacteria on Glaciers in West Greenland." *Polar Science* 4(1):71-80.
- Uno, I., K. Eguchi, K. Yumimoto, T. Takemura, A. Shimizu, M. Uematsu, Z. Liu, Z. Wang, Y. Hara, and N. Sugimoto. 2009. "Asian Dust Transported One Full Circuit around the Globe." *Nature Geoscience* 2(8):557.
- Weil, T., C. De Filippo, D. Albanese, C. Donati, M. Pindo, L. Pavarini, F. Carotenuto, M. Pasqui, L. Poto, J. Gabrieli, and C. Barbante. 2017. "Legal Immigrants: Invasion of Alien Microbial Communities during Winter Occurring Desert Dust Storms." *Microbiome* 5(1):32. doi:10.1186/s40168-017-0249-7.
- Weir-Brush, J. R., V. H. Garrison, G. W. Smith, and E. A. Shinn. 2004. "The Relationship between Gorgonian Coral (Cnidaria: Gorgonacea) Diseases and African Dust Storms." *Aerobiologia* 20(2):119-126.
- Wickham, H. 2016. *ggplot2: Elegant Graphics for Data Analysis*. 2d ed. New York, NY: Springer Nature Switzerland AG.
- Wunderlin, T., B. Ferrari, and M. Power. 2016. "Global and Local-Scale Variation in Bacterial Community Structure of Snow from the Swiss and Australian Alps." *FEMS Microbiology Ecology* 92(9):fiw132,1-12. doi:10.1093/femsec/fiw132.

## Acronyms and Abbreviations

<b>Term</b>	<b>Definition</b>
AGL	Above Ground Level
ANOVA	Analysis of Variance
ARTEMIS STO-R	Army Terrestrial-Environmental Modeling and Intelligence System Science Technology Objective-Research
BLAST	Building Loads Analysis and System Thermodynamics
BPSS	Berthoud Pass Summit Site
CAIC	Colorado Avalanche Information Center
CODOS	Colorado Dust-on-Snow
CRREL	Cold Regions Research and Engineering Laboratory
CSAS	Center for Snow and Avalanche Studies
CT	Current Transformer
DNA	Deoxyribonucleic Acid
DUST-CLOUD	Dynamic Undisturbed Soils Testbed to Characterize Local Origins and Uncertainties of Dust
EPOLAR	Engineering for Polar Operations, Logistics, and Research
ERDC	U.S. Army Engineer Research and Development Center
ERDC-CRREL	Engineer Research and Development Center, Cold Regions Research and Engineering Laboratory
FEMS	Facility Equipment Maintenance System
GDAS	Global Data Assimilation System
GRE	Geospatial Research Engineering
HS	Height-of-Snow
HYSPLIT	Hybrid Single Particle Lagrangian Integrated Trajectory
ID	Identification
METAR	Meteorological Terminal Aviation Routine
N/A	Not Applicable
NA	Nutrient Agar
NIR	Near Infrared
NOAA	National Oceanic and Atmospheric Administration
NWCC	National Water and Climate Center
OTU	Operational Taxonomic Unit
PCoA	Principal Coordinates Analysis
PTSP	Putney Study Plot
QIIME	Quantitative Insights Into Microbial Ecology
R2A	Reasoner's Agar
S/V	Surface-Area to Volume
SASP	Swamp Angel Study Site
SBB	Senator Beck Basin
SBSG	Senator Beck Stream Gauge

---

<b>Term</b>	<b>Definition</b>
SBSP	Senator Beck Study Plot
SF	Standard Form
TR	Technical Report
TSA	Trypticase Soy Agar
UTC	Coordinated Universal Time
UV	Ultraviolet

# Appendix A: Meteorology of the Senator Beck Basin

## A.1 Wind data

Table A-1. PTSP wind data.

Event ID	# of Hours	Avg. Resultant Wind Speed (m s <sup>-1</sup> )	Avg. Wind Direction (Cardinal Degrees)	Peak Wind Gust (m s <sup>-1</sup> )
D1	23 Hours	17.87	218°	81.10
D2	19 Hours	11.68	203°	66.59
D3	15 Hours	10.66	178°	64.01
D4	21 Hours	13.40	231°	61.33

Figure A-1. PTSP wind data for event D1. Average wind speed and cardinal direction were 17.87 m s<sup>-1</sup> and 218 degrees, respectively.

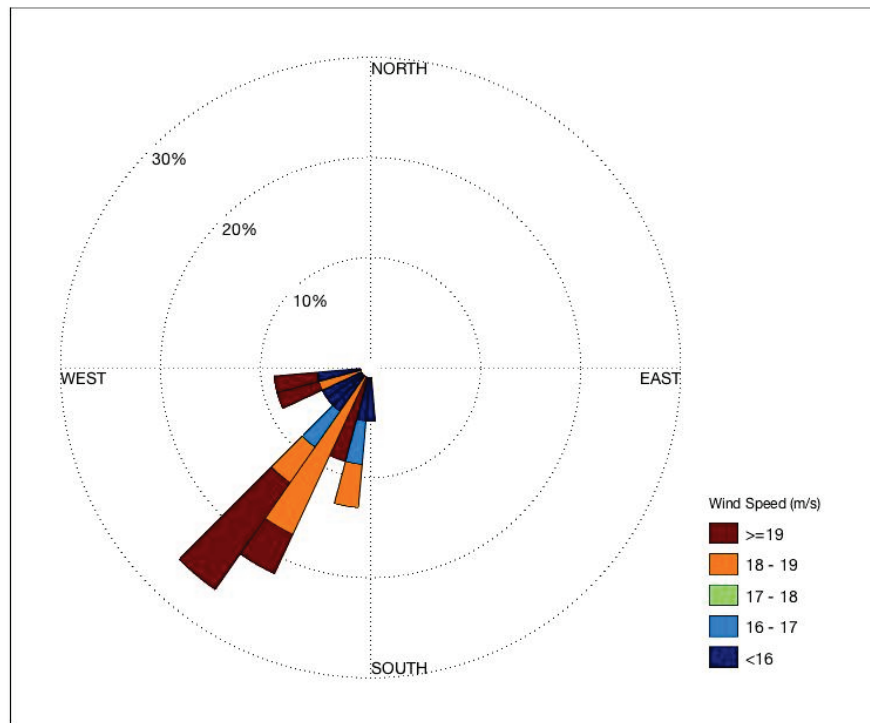


Figure A-2. PTSP wind data for event D2. Average wind speed and cardinal direction were 11.68 m s<sup>-1</sup> and 203 degrees, respectively.

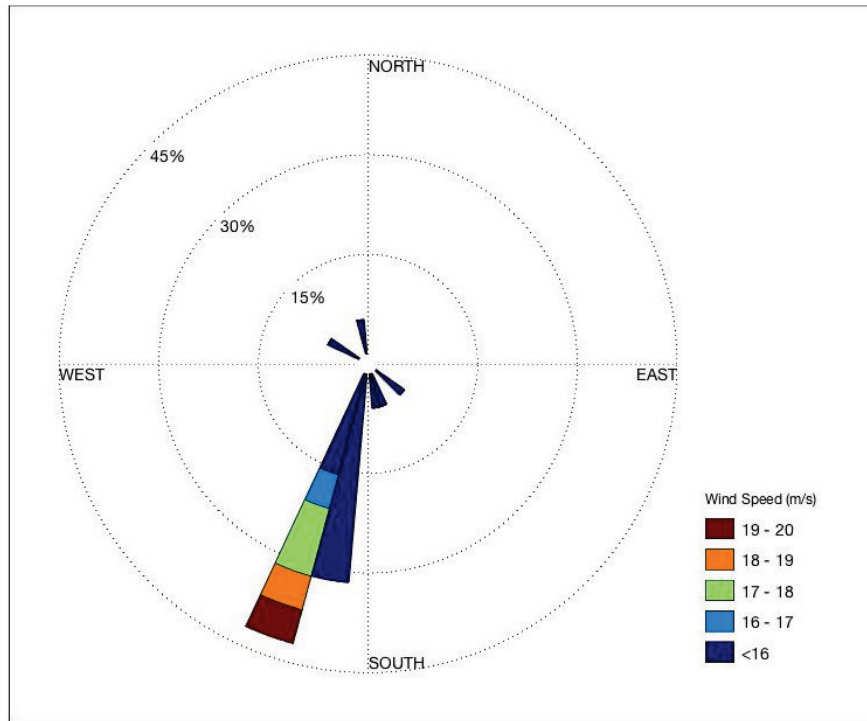


Figure A-3. PTSP wind data for event D3. Average wind speed and cardinal direction were 10.66 m s<sup>-1</sup> and 178 degrees, respectively.

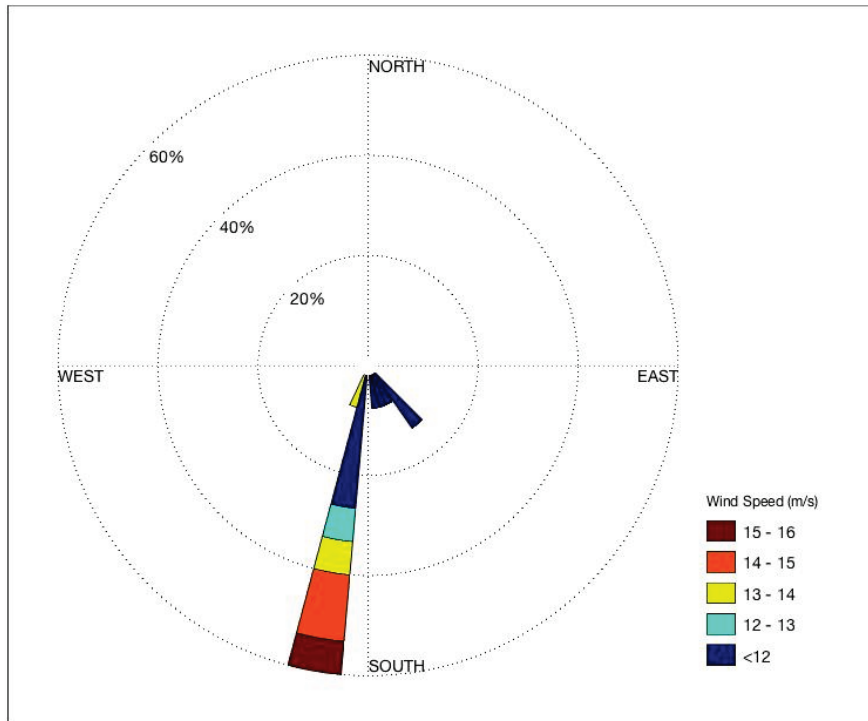


Figure A-4. PTSP wind data for event D4. Average wind speed and cardinal direction were 13.40 m s<sup>-1</sup> and 231 degrees, respectively.

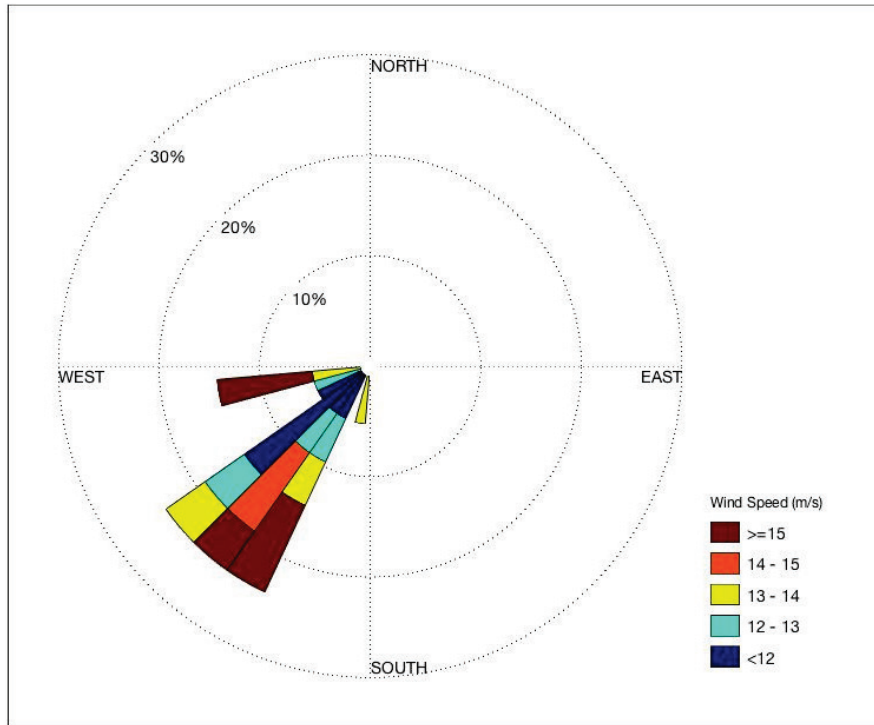


Table A-2. SBSP wind data.

Event ID	# of Hours	Avg. Resultant Wind Speed (m s <sup>-1</sup> )	Avg. Wind Direction (Cardinal Degrees)	Peak Wind Gust (m s <sup>-1</sup> )
D1	23 Hours	10.38	266°	53.07
D2	19 Hours	5.45	197°	17.66
D3	15 Hours	5.61	173°	18.46
D4	21 Hours	6.92	256°	27.06

Figure A-5. SBSP wind data for event D1. Average wind speed and cardinal direction were 10.38 m s<sup>-1</sup> and 266 degrees, respectively.

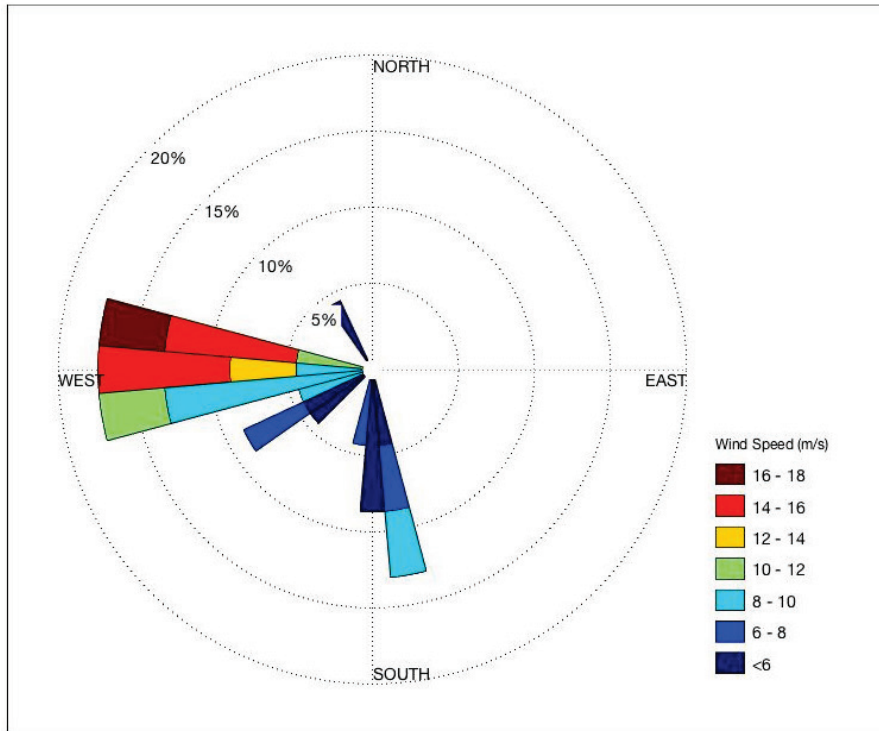


Figure A-6. SBSP wind data for event D2. Average wind speed and cardinal direction were 5.45 m s<sup>-1</sup> and 197 degrees, respectively.

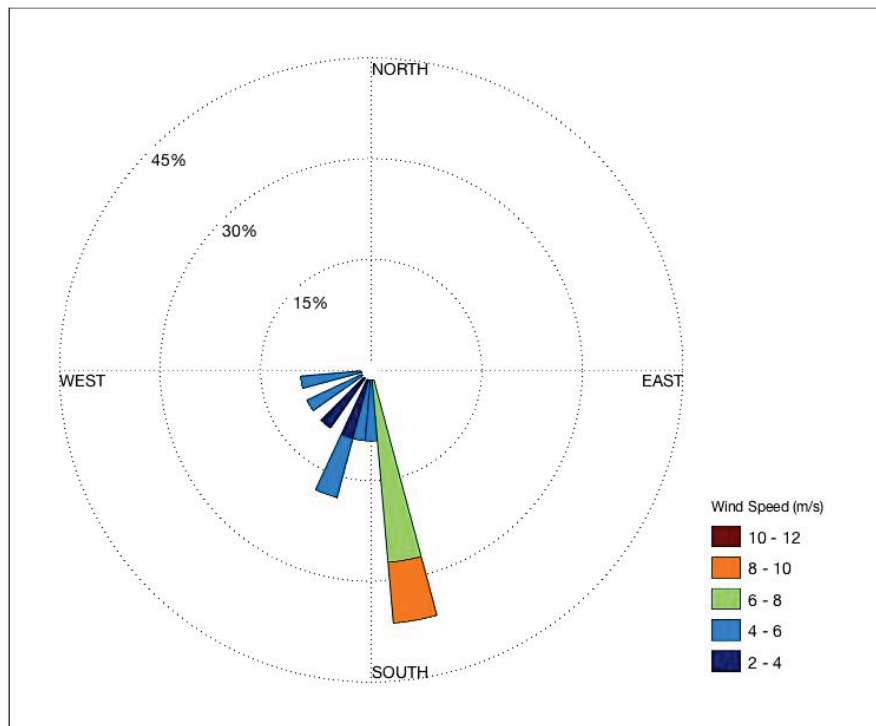




Figure A-7. SBSP wind data for event D3. Average wind speed and cardinal direction were 5.61 m s<sup>-1</sup> and 173 degrees, respectively.

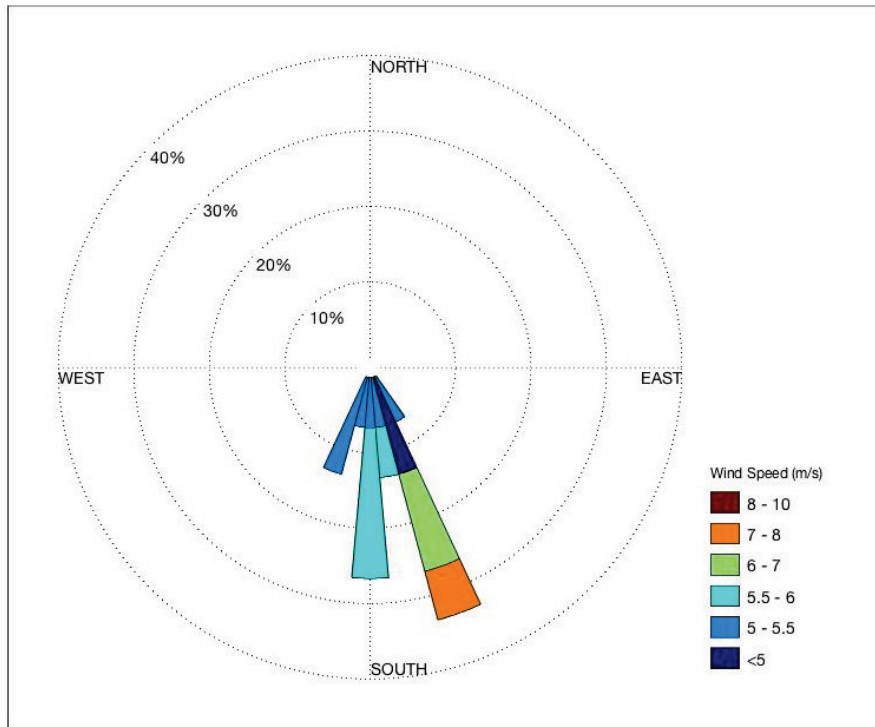


Figure A-8. SBSP wind data for event D4. Average wind speed and cardinal direction were 6.92 m s<sup>-1</sup> and 256 degrees, respectively.

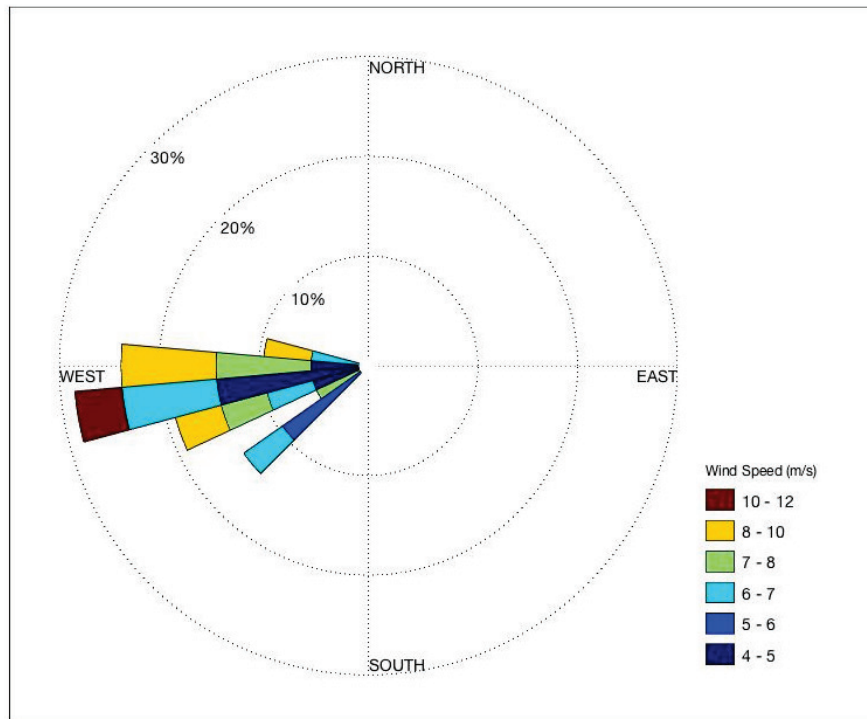


Figure A-9. Data incorporating specific wind rose diagrams and wind speeds from the SBSP.

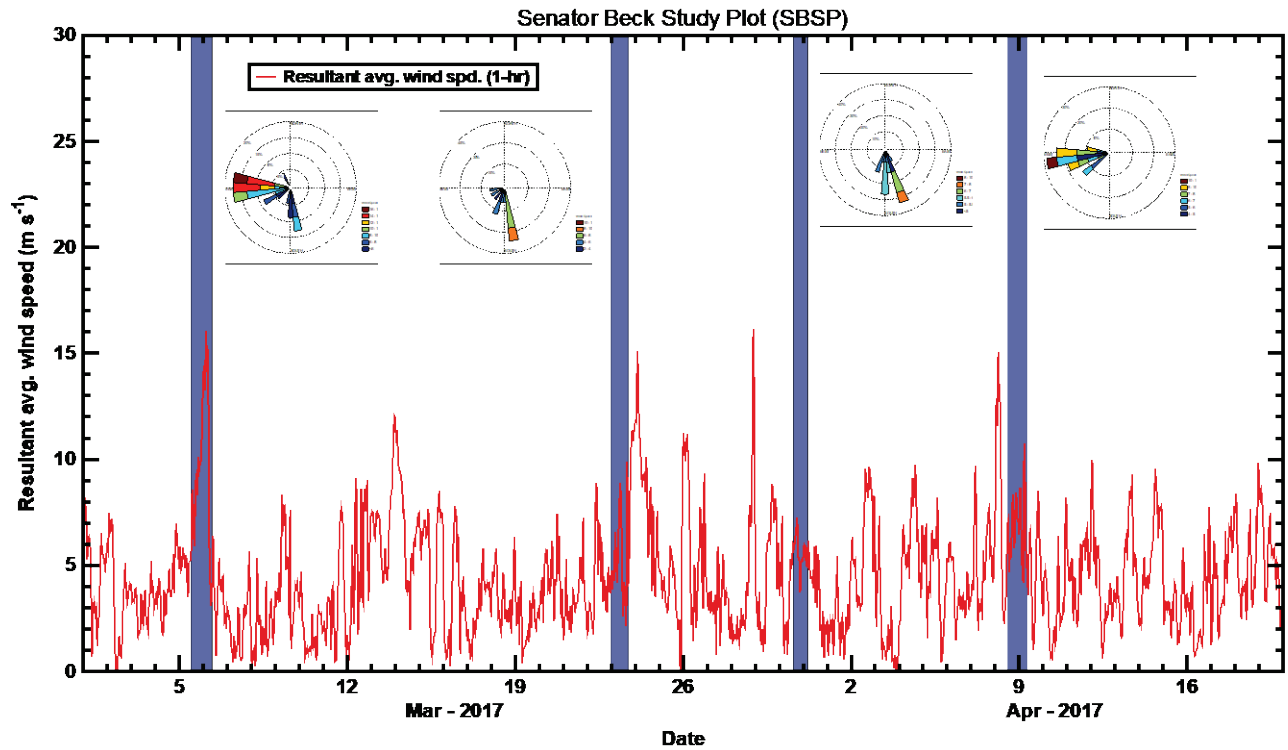


Table A-3. SASP wind data.

Event ID	# of Hours	Avg. Resultant Wind Speed (m s <sup>-1</sup> )	Avg. Wind Direction (Cardinal Degrees)	Peak Wind Gust (m s <sup>-1</sup> )
D1	23 Hours	3.08	246°	17.64
D2	19 Hours	1.21	255°	9.47
D3	15 Hours	0.88	247°	6.20
D4	21 Hours	2.55	253°	9.01

Figure A-10. SASP wind data for event D1. Average wind speed and cardinal direction were 3.08 m s<sup>-1</sup> and 246 degrees, respectively.

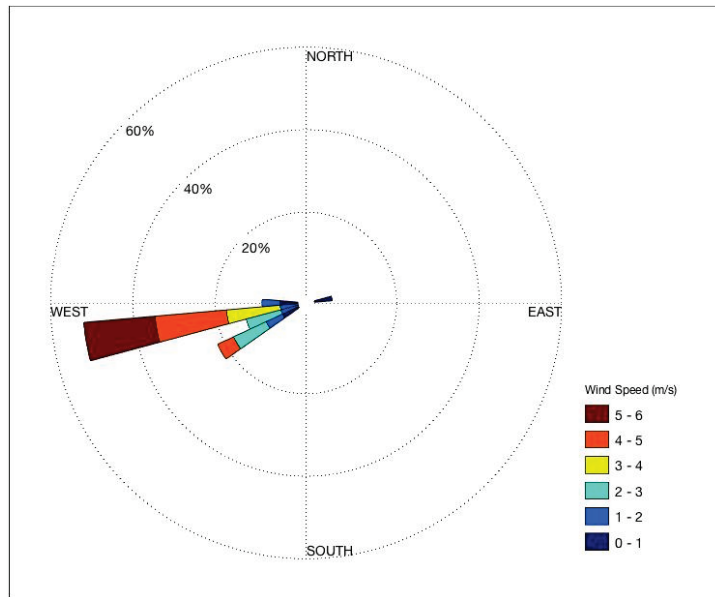


Figure A-11. SASP wind data for event D2. Average wind speed and cardinal direction were 1.21 m s<sup>-1</sup> and 255 degrees, respectively.

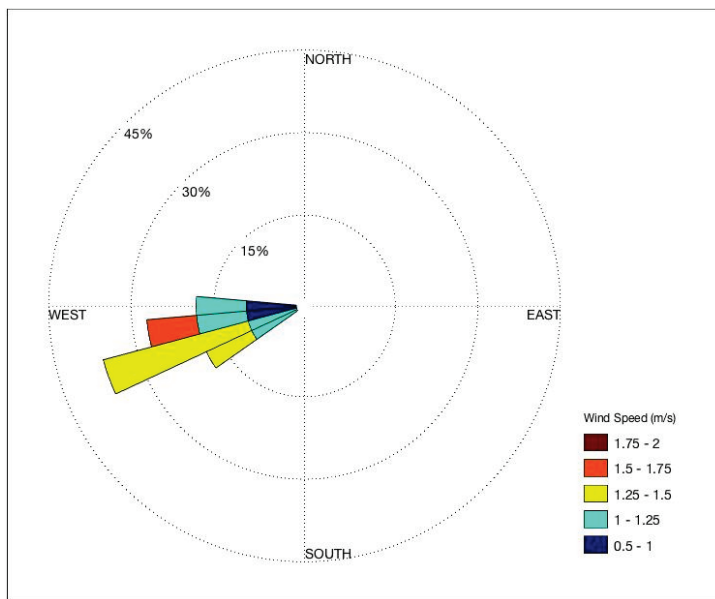


Figure A-12. SASP wind data for event D3. Average wind speed and cardinal direction were 0.88 m s<sup>-1</sup> and 247 degrees, respectively.

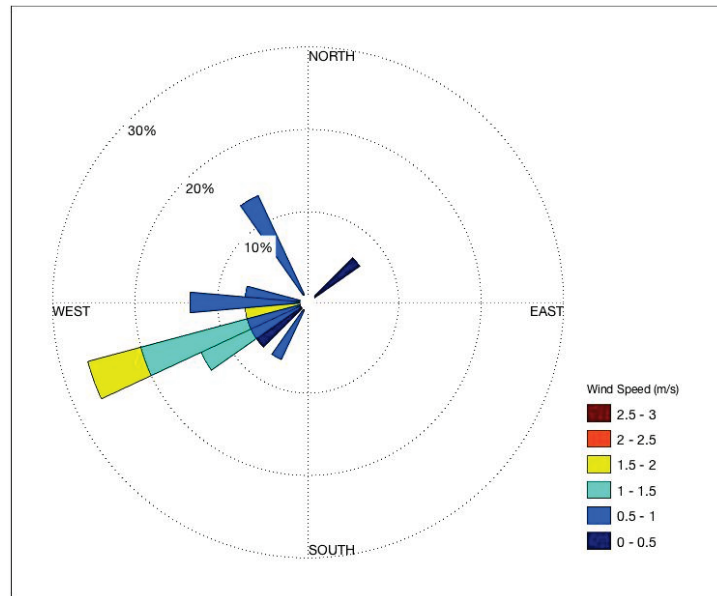


Figure A-13. SASP wind data for event D4. Average wind speed and cardinal direction were 2.55 m s<sup>-1</sup> and 253 degrees, respectively.

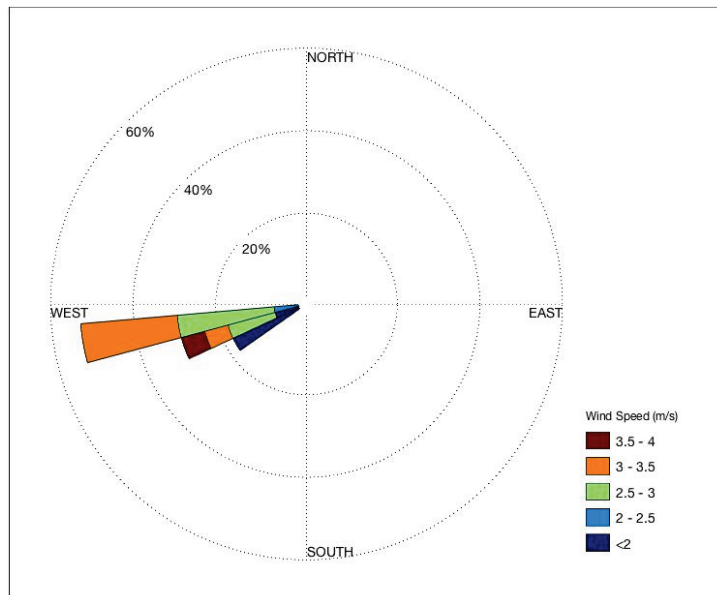


Figure A-14. Data from incorporating specific wind rose diagrams and wind speeds over time at SASP.

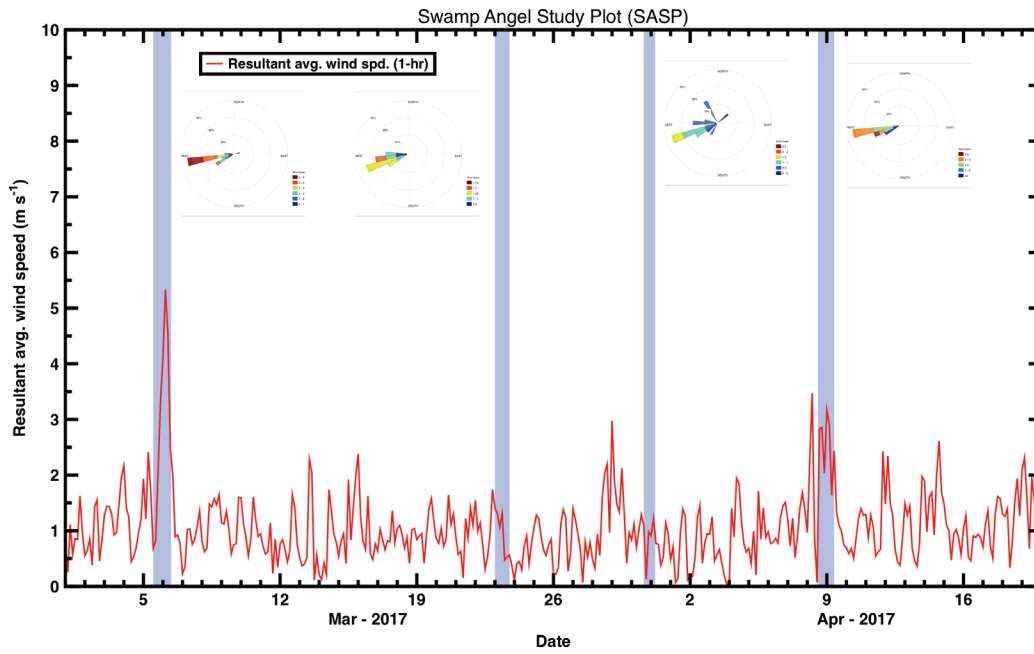


Table A-4. Average wind direction for all event over each study plot station

Event ID	PTSP - Avg. Wind Dir. (Cardinal Degrees)	SBSP - Avg. Wind Dir. (Cardinal Degrees)	SASP - Avg. Wind Dir. (Cardinal Degrees)
ALL Events	207.5°	223°	250.25°

### A.2 Additional HYSPLIT model runs (simulation runs)

Figure A-15. NOAA HYSPLIT model, backward trajectories ending at 1800 Coordinated Universal Time (UTC) 06 Mar 17 (GDAS Meteorological Data).

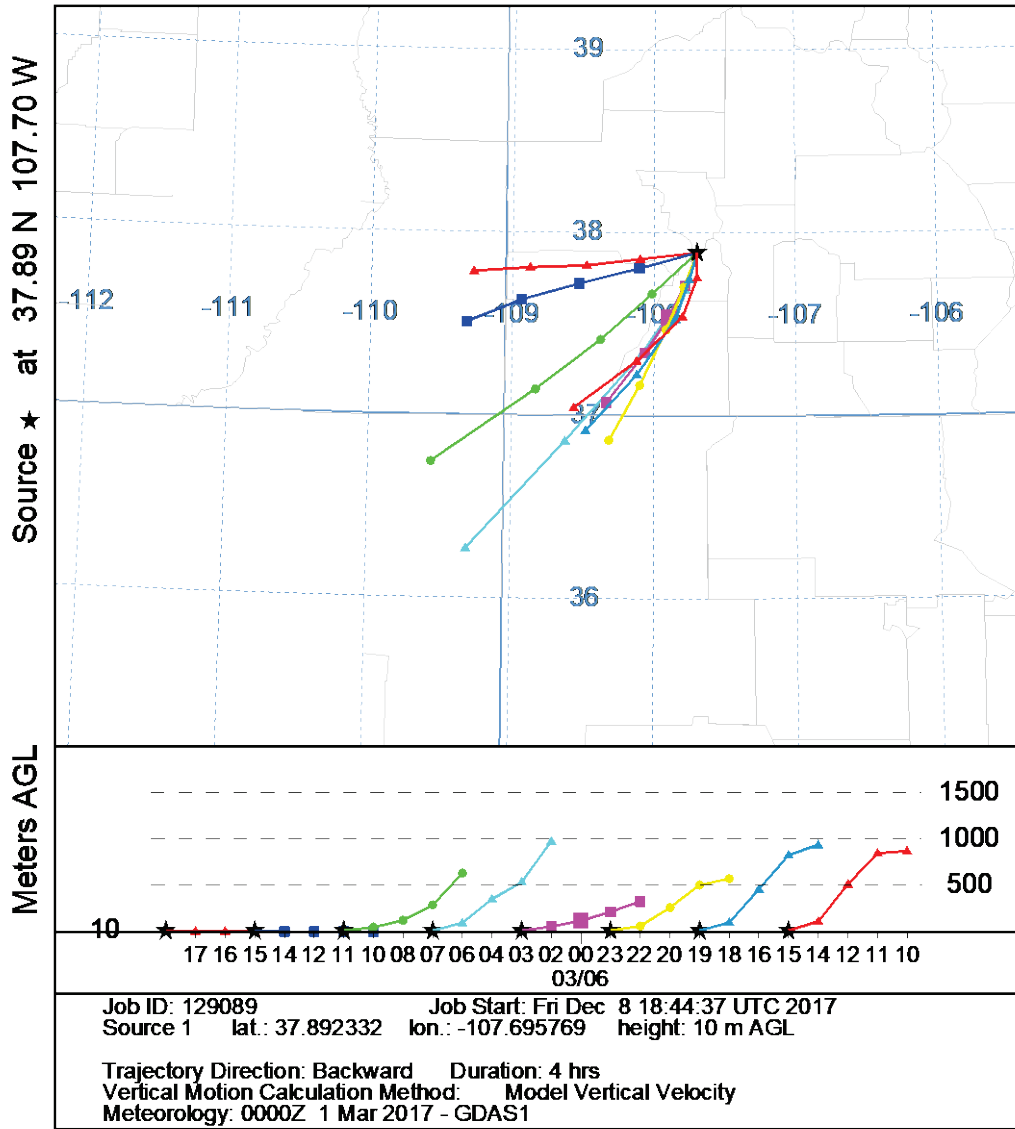


Figure A-16. NOAA HYSPLIT model, backward trajectories ending at 2200 UTC 23 Mar 17 (GDAS Meteorological Data).

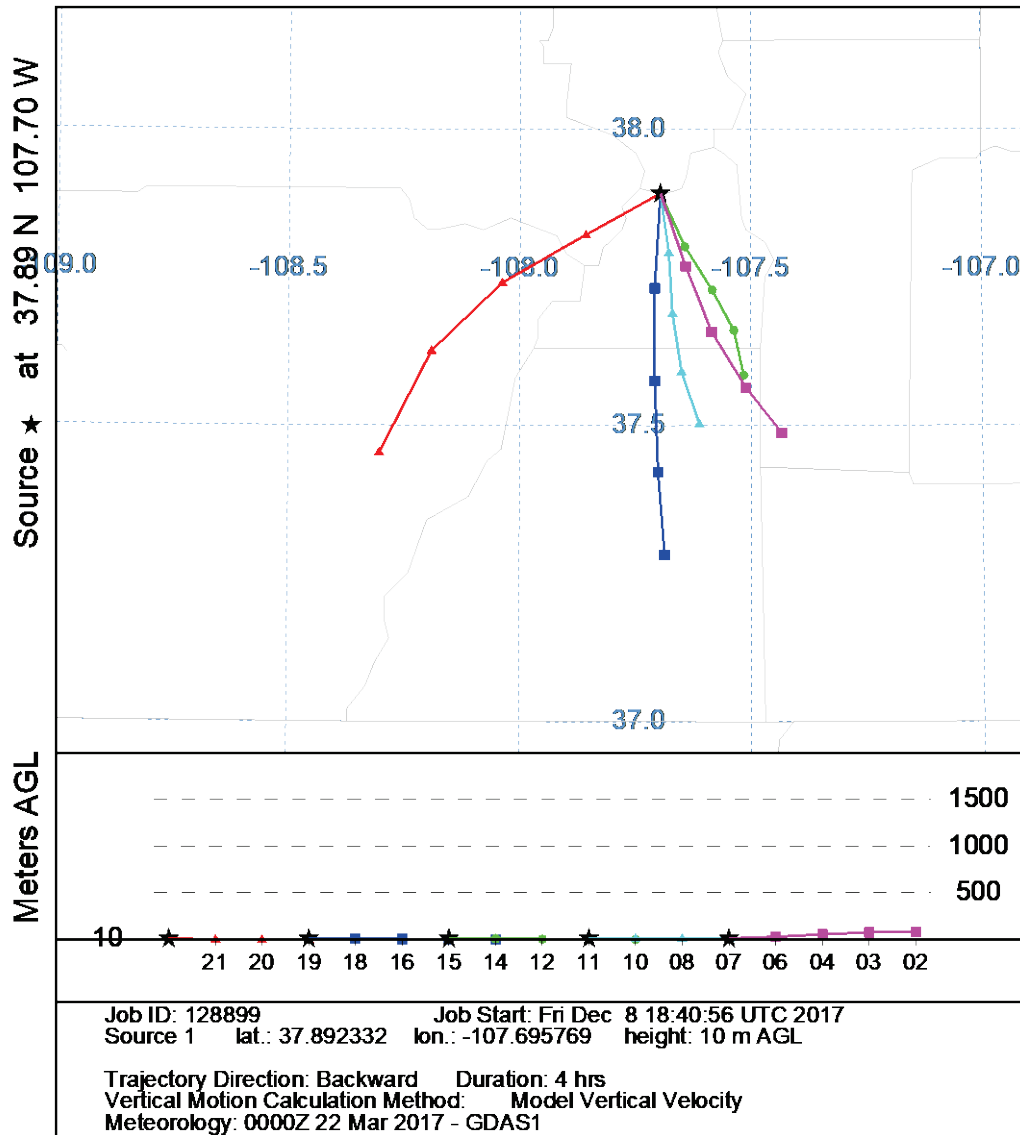


Figure A-17. NOAA HYSPLIT model, backward trajectories ending at 1400 UTC 31 Mar 17 (GDAS Meteorological Data).

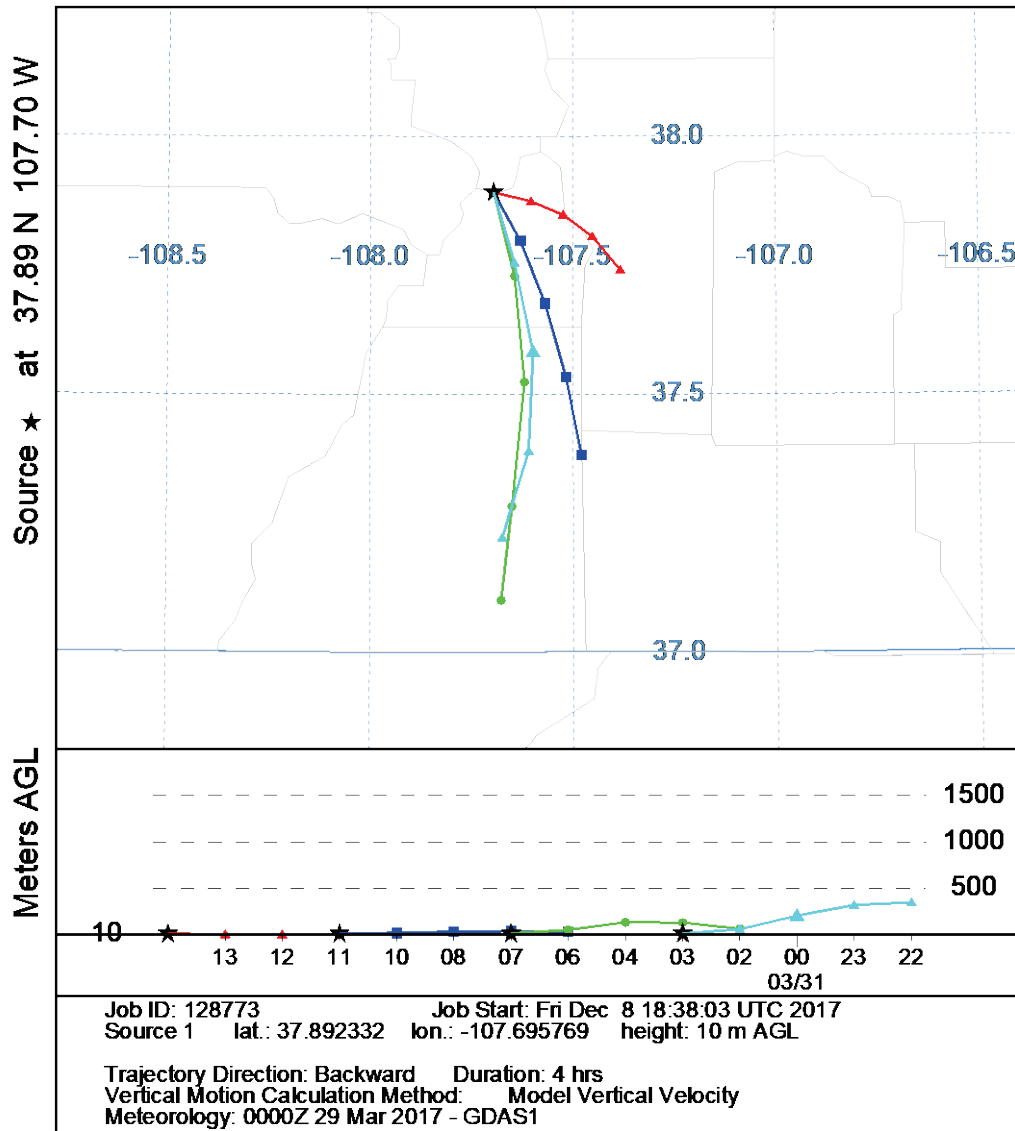
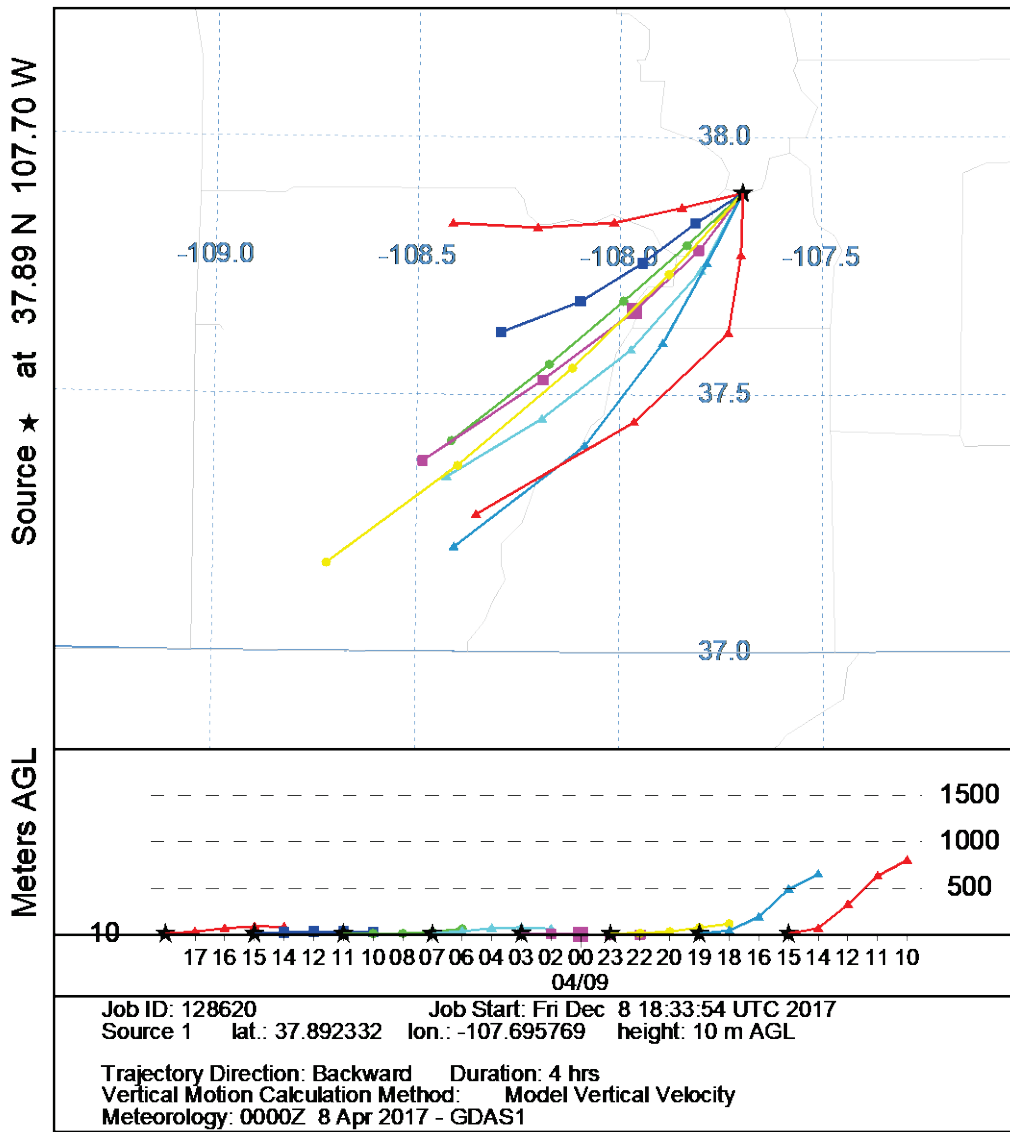




Figure A-18. NOAA HYSPLIT model, backward trajectories ending at 1800 UTC 09 Mar 17 (GDAS Meteorological Data).



# REPORT DOCUMENTATION PAGE

Form Approved  
OMB No. 0704-0188

Public reporting burden for this collection of information is estimated to average 1 hour per response, including the time for reviewing instructions, searching existing data sources, gathering and maintaining the data needed, and completing and reviewing this collection of information. Send comments regarding this burden estimate or any other aspect of this collection of information, including suggestions for reducing this burden to Department of Defense, Washington Headquarters Services, Directorate for Information Operations and Reports (0704-0188), 1215 Jefferson Davis Highway, Suite 1204, Arlington, VA 22202-4302. Respondents should be aware that notwithstanding any other provision of law, no person shall be subject to any penalty for failing to comply with a collection of information if it does not display a currently valid OMB control number. PLEASE DO NOT RETURN YOUR FORM TO THE ABOVE ADDRESS.

<b>1. REPORT DATE (DD-MM-YYYY)</b> March 2021	<b>2. REPORT TYPE</b> Final Technical Report (TR)	<b>3. DATES COVERED (From - To)</b>
--	--	-------------------------------------

<b>4. TITLE AND SUBTITLE</b> Microscale Dynamics between Dust and Microorganisms in Alpine Snowpack	<b>5a. CONTRACT NUMBER</b>
	<b>5b. GRANT NUMBER</b>
	<b>5c. PROGRAM ELEMENT</b>

<b>6. AUTHOR(S)</b> Alison K. Thurston, Zoe R. Courville, Lauren B. Farnsworth, Ross Lieblappen, Shelby A. Rosten, John M. Fegyveresi, Stacey J. Doherty, Robert M. Jones and Robyn A. Barbato	<b>5d. PROJECT NUMBER</b> K8B968
	<b>5e. TASK NUMBER</b>
	<b>5f. WORK UNIT NUMBER</b> T42 053HJo, AT24 L6620L

<b>7. PERFORMING ORGANIZATION NAME(S) AND ADDRESS(ES)</b> U.S. Army Engineer Research and Development Center (ERDC) Cold Regions Research and Engineering Laboratory (CRREL) 72 Lyme Road, Hanover, NH 03755-1290	<b>8. PERFORMING ORGANIZATION REPORT NUMBER</b>  ERDC/CRREL TR-20-12
---	--

<b>9. SPONSORING / MONITORING AGENCY NAME(S) AND ADDRESS(ES)</b> Headquarters, U.S. Army Corps of Engineers (HQUSACE) 441 G St., NW Washington, DC 20314-1000	<b>10. SPONSOR/MONITOR'S ACRONYM(S)</b>
	<b>11. SPONSOR/MONITOR'S REPORT NUMBER(S)</b>

**12. DISTRIBUTION / AVAILABILITY STATEMENT**  
Approved for public release; distribution is unlimited.

**13. SUPPLEMENTARY NOTES**  
6.1 (Basic Research); 6.2 (Applied Research); Funding Account Number U4357509; Funding Account Number U4363500

**14. ABSTRACT**

Dust particles carry microbial and chemical signatures from source regions to deposition regions. Dust and its occupying microorganisms are incorporated into, and can alter, snowpack physical properties including snow structure and resultant radiative and mechanical properties that in turn affect larger-scale properties, including surrounding hydrology and maneuverability. Microorganisms attached to deposited dust maintain genetic evidence of source substrates and can be potentially used as bio-sensors.

The objective of this study was to investigate the impact of dust-associated microbial deposition on snowpack and microstructure. As part of this effort, we characterized the microbial communities deposited through dust transport, examined dust provenance, and identified the microscale location and fate of dust within a changing snow matrix.

We found dust characteristics varied with deposition event and that dust particles were generally embedded in the snow grains, with a small fraction of the dust particles residing on the exterior of the snow matrix. Dust deposition appears to retard expected late season snow grain growth. Both bacteria and fungi were identified in the collected snow samples.

**15. SUBJECT TERMS**  
Dust, Microorganisms, Geospatial data, Snow

<b>16. SECURITY CLASSIFICATION OF:</b>			<b>17. LIMITATION OF ABSTRACT</b>  SAR	<b>18. NUMBER OF PAGES</b>  58	<b>19a. NAME OF RESPONSIBLE PERSON</b>
<b>a. REPORT</b> Unclassified	<b>b. ABSTRACT</b> Unclassified	<b>c. THIS PAGE</b> Unclassified			<b>19b. TELEPHONE NUMBER (include area code)</b>